THE DIFFUSION OF IMPURITIES IN MAGNESIUM OXIDE

A thesis submitted for the degree of Master of Science

by

B.C. Harding, B.Sc., B.A. (Oxon).

Department of Physics,

Australian National University.

1967.

The work contained in this thesis is my own except where another source is indicated.

B. C. Harding

Contents

List of figures

ACKNOWLEDGMENTS

Thanks are due to Professor D.N.F. Dunbar, Head of the Department of Physics, and to Drs. A.J. Mortlock and R.J. MacDonald for helpful discussions and guidance throughout the course of this investigation. Mr. D.M. Price gave valuable technical assistance and Mr. Ken Smith is thanked for his photographic work. In addition, the financial support provided by the Australian Atomic Energy Commission is gratefully acknowledged.

Abstract

The diffusion of Ca, Be and Ba in MgO single crystals has been studied in the temperature range 1000°C and 1700°C. In the case of Ca, a single experiment was conducted using a previously described autoradiographic technique as a check on earlier results. Be and Ba diffusion was investigated using a sectioning method. The temperature dependence of measured diffusion coefficients is given by the Arrhenius Equation

$$D = D_o \exp(-Q/kT)$$

where k is Boltzmanns constant in eV/°K and T is the absolute temperature.

For Be, the activation energy Q was found to be 1.6 eV and D_o, 1.41×10^{-5} cm^2/sec. For Ba, the diffusion profiles consisted of two parts and two Arrhenius equations were required to describe the results. The diffusion parameters in this case were (i) 3.38 eV and 0.07 cm^2/sec and (ii) 1.85 eV and 6.3×10^{-5} cm^2/sec, respectively. These results do not agree with the predictions of a previously proposed correlation between the activation energy and the ratio of the radius to the electronic polarisability of the diffusing ion.

The Ba results indicate that dislocations can have a strong influence on measured diffusion coefficients. This

conclusion is supported by the results of early experiments on the diffusion of Ni in MgO and recent results of measurements of Ca diffusion in MgO. Further evidence has been derived from photomicrography and general considerations drawn from established results of diffusion studies in metals.

I. INTRODUCTION

1.1. General Comments on Diffusion in Solids

1.1.1. "Normal" Diffusion, with Reference to Metals

Diffusion studies until recent years have been conducted almost exclusively on metals. Atomic defects in metal lattices are fairly well understood and various diffusion mechanisms have been shown to be possible. With the use of radio-active tracers of high purity and careful sectioning techniques, it has become possible to make reproducible measurements of diffusion coefficients for a large number of systems. Many of the apparently anomalous results of twenty years ago have been corrected and many of the mechanisms invoked to explain them are no longer necessary. The lattice vacancy has emerged as the defect most commonly responsible for "lattice" diffusion in pure monatomic materials. Diffusion by an interstitial mechanism is less common but has been shown to apply, for example, to the diffusion of C in α-Fe (Wert, 1950), C in Ta (Powers and Doyle, 1959) and O in Ge and Si (Haas, 1960). The parameters characteristic of "normal" diffusion in metals fit well-known empirical correlations. Activation energies (Q cals) for self-diffusion are related to the melting point of the metal, T_m, and the latent heat of fusion, L_m, by the following equations:-

$$Q = 34\ T_m \qquad \ldots\ldots \quad (1\text{-}1)$$

and $$Q = 16.5\, L_m \qquad \ldots\ldots \quad (1\text{-}2)$$

The temperature dependence of both self-diffusion coefficients and impurity diffusion coefficients is described by the Arrhenius equation

$$D = D_o \exp(-Q/RT) \qquad \ldots\ldots \quad (1\text{-}3)$$

where T is the absolute temperature and R is the gas constant. Activation energies are usually of the order of 50 K cals $mole^{-1}$ and D_o, the "frequency" or "pre-exponential" factor, lies within an order of magnitude of 0.5 $cm^2\ sec^{-1}$.

The justification of equation (1-3) is derived from models based on the Wigner-Eyring theory of absolute reaction rates. The diffusion coefficient is expressed as

$$D = \gamma a^2 p_d \nu_j \qquad \ldots\ldots \quad (1\text{-}4)$$

where γ is a constant of about unity, a is the lattice parameter, p_d is the probability that a defect exists adjacent to a diffusing atom and ν_j is the jump frequency. For a random distribution of defects, p_d is equal to their relative concentration. Then

$$p_d = \exp(-\Delta G_f/RT) \qquad \ldots\ldots \quad (1\text{-}5)$$

where ΔG_f is the increase in Gibbs free energy required to form a mole of defects. In the Wert and Zener treatment, (1949), ν_j is derived from a simplified model for the jump

process. The jump is considered to be equivalent to the reversible motion of an atom across a potential barrier of height W, in thermal equilibrium, while the atom, vibrating with a constant frequency ν_o, is constrained to a plane perpendicular to the direction of motion. Then the barrier height W is the isothermal, isobaric work required for traversal and can be equated to an increment in Gibbs free energy ΔG_m. Thus

$$\nu_j = \nu_o \exp(-\Delta G_m/RT) \quad \ldots\ldots \quad (1\text{-}6)$$

Combining equations (1-4), (1-5) and (1-6) we obtain

$$D = \gamma a^2 \nu_o \exp\left[-(\Delta G_f + \Delta G_m)/RT\right] \quad \ldots\ldots \quad (1\text{-}7)$$

and using the thermodynamic relation $\Delta G = \Delta H - T\Delta S$ where H is enthalpy and S entropy, we arrive at

$$D = \gamma a^2 \nu_o \exp\left[(\Delta S_f + \Delta S_m)/R\right] \exp\left[-(\Delta H_f + \Delta H_m)/RT\right] \quad \ldots\ldots \quad (1\text{-}8)$$

Comparing this with equation (1-3) we see that

$$D_o = \gamma a^2 \nu_o \exp\left[(\Delta S_f + \Delta S_m)/R\right]$$

$$\text{and} \quad Q = (\Delta H_f + \Delta H_m) \quad \ldots\ldots \quad (1\text{-}9)$$

If ν_o is assumed to be the Debye frequency, say 5×10^{12} sec^{-1}, the "normal" values of D_o lead to a positive value of $(\Delta S_f + \Delta S_m)$. This derivation cannot be regarded as rigorous. A far more acceptable approach has been given by Vineyard (1957), but this will not be detailed here.

1.1.2. Diffusion in Ionic Solids

In the study of ionic solids, the alkali halides have been the subject of many investigations. In particular, the relation between electrical conductivity and diffusion is fairly well understood and has been applied successfully to a number of systems (Shewmon, 1963, p.140). This relation is usually expressed in the form of the Nernst-Einstein equation

$$\frac{\sigma_A}{D_A} = \frac{N_A e^2}{kT} \qquad \ldots\ldots \quad (1\text{-}10)$$

where σ_A is the contribution of ion type A to the electrical conductivity, N_A is the number of A ions per cm^3, e is the ion charge and D_A is the self-diffusion coefficient for A. Actually, a factor f should be introduced to account for the correlation between the directions of successive jumps of the diffusing ion (Barr and Le Claire, 1964).

An important factor influencing diffusion in purely ionic solids is the impurity concentration. This can be illustrated by quoting the results of Mapother, Crooks and Maurer (1950) for the self diffusion of Na in NaCl. It was found that the Arrhenius plot (log D vs 1/T) showed a discontinuity at a temperature of about 550°C. In the high temperature region, the values of Q and D_o were given as 1.8 eV (41.6 K cals) and 3.1 cm^2 sec^{-1} respectively, and for low temperatures, they were found to be 0.77 eV (17.8 K cals) and 1.6×10^{-6} cm^2 sec^{-1}. The presence of divalent impurity

ions can explain these results. In order to preserve electrical neutrality, every divalent impurity on an Na^+ site gives rise to a cation vacancy. At high temperatures, in the "intrinsic region", thermally produced vacancies dominate and the activation energy includes the enthalpy of formation of the defect and the enthalpy of movement of the diffusing ion. At low temperatures, the concentration of vacancies is nearly constant and equal to the concentration of divalent impurities. The activation energy then only consists of the enthalpy of motion of the ion and hence is less than the Q for the intrinsic range. This region is called the "extrinsic range". That this theory is correct is indicated by the work done with "doped" crystals (e.g. Kelting and Witt, 1949). It is found that increasing the mole fraction of impurity causes the diffusion coefficients in the extrinsic region to increase, but the activation energy for diffusion in a given crystal is unaltered. Above a certain temperature, which increases slowly with impurity content, the same intrinsic diffusion parameters are obtained for all samples irrespective of impurity concentration. It has also been concluded that neutral vacancy-impurity complexes are formed to some extent, since the diffusion coefficients calculated from conductivity measurements are too low compared with measured values of D, indicating that species are taking part in diffusion which do not contribute to conduction.

So far, little has been accomplished in the study of diffusion in oxides. A perusal of a bibliographical review of self-diffusion in metal oxides (Cumming and Harrop, 1965) indicates that much of the early work covered very small temperature ranges. No attempt seems to have been made to co-ordinate results, and often there are wide discrepancies between data obtained by various authors. Interest in diffusion processes in oxides was fostered by their use in atomic reactors. Uranium and Thorium oxides are of interest because of their use as fuel for reactors, and beryllium oxide, because of its attractive nuclear properties such as low absorption cross section for neutrons, has been studied with the intention of using it as a moderator, and as a matrix in which to suspend fuel particles. Diffusion of fission products such as Xe, Kr and I in poly-crystalline compacts of BeO is of importance because by this process the reactor coolant could become contaminated. Such sources as Nuclear Science Abstracts reveal many references to these studies (e.g. Morrison, 1963/4).

As in the case of the alkali halides, it might be expected that impurities would effect lattice diffusion in oxides, but so far as is known, no systematic study of this aspect has been made. Mitoff (1959) proposed that iron played a considerable part in determining conductivity in MgO and in a later paper (Mitoff, 1962) studied the effect of

lithium doping in the same material. Wuensch and Vasilos (1962) measured the coefficients for Ni^{2+} diffusing in two MgO samples containing 35 ppm and 75 ppm of iron respectively. The more impure specimen showed an increase of 20% in the diffusion coefficient and the authors state that within the accuracy of their analyses, this is the increase to be expected if the presence of impurities with valence greater than two caused additional cation vacancies.

Other factors that can effect diffusion in oxides are the atmosphere in which annealing is carried out, and the departure of the crystal from stochiometry. A well-studied example of the latter effect is the FeO phase of the iron-oxygen system (Himmel, Mehl and Birchenall, 1953). An example of the effect of the annealing atmosphere on diffusion is found in the work on Co self-diffusion in CoO (Carter and Richardson, 1954). The variation of vacancy concentration with oxygen partial pressure can be obtained from the equation

$$2Co^{2+} + \tfrac{1}{2} O_2 \rightleftharpoons 2Co^{3+} + V_{Co} + O^{2-} \qquad \ldots\ldots \quad (1\text{-}11)$$

where V_{Co} is a cation vacancy. Introducing the concept of an "electron hole" ($\oplus$) to describe an electron deficit, this equation can be written as

$$\tfrac{1}{2} O_2 \rightleftharpoons 2\oplus + V_{Co} + O^{2-} \qquad \ldots\ldots \quad (1\text{-}12)$$

Applying chemical thermodynamics to equation (1-12), it can be

deduced that this system gives rise to a pressure dependence of the diffusion coefficient given by

$$D \propto P_{O_2}^{1/6} \qquad \ldots\ldots \quad (1\text{-}13)$$

In fact, the diffusion coefficient was found to increase with approximately the 1/3rd power of P_{O_2} and it was suggested that some degree of interaction between vacancies and electron holes would account for this departure from simple theory. Pappis and Kingery (1961) found that Al_2O_3 was a p-type semiconductor, and that the conductivity depended on oxygen partial pressure. Paladino and Kingery (1962) noted that diffusion coefficients could be similarly dependent due to the non-stochiometric formation of lattice vacancies, and suggested a reaction such as:-

$$\tfrac{3}{4}\, O_2 = \tfrac{3}{2}\, O^{2-}\,(\text{lattice}) + Al^{3+}(\text{vac.}) + 3\,\oplus \qquad \ldots\ldots \quad (1\text{-}14)$$

Conductivity measurements on MgO (Mitoff, 1959, 1962, 1964) have indicated that similar results could be expected in this material, but Wuensch and Vasilos (1962) claim that no difference was noted between impurity diffusion coefficients measured in two different atmospheres.

1.2. Diffusion in MgO

1.2.1. Self-Diffusion and Electrical Conductivity

Because its structure is similar to that of several of the alkali halides, MgO provides a good starting point for

a systematic study of diffusion in oxides. Before comparisons between impurity diffusion rates in different solvents can be made, the relative diffusion rates of a range of impurities in a single solvent should be measured in an attempt to reveal the factors governing diffusion mechanisms in the simpler case. As far as is known, only MgO has been studied with this object in mind. Cation self-diffusion was measured over the temperature range 1400-1600°C using ^{28}Mg as tracer (Lindner and Parfitt, 1957). Both "surface activity decrease" and sectioning techniques were used, but the short half life of the isotope restricted the temperature range. To obtain a measurable penetration below 1400°C would have required too long an annealing time. The activation energy was quoted as 3.43 eV and D_o was found to be 0.249 cm^2 sec^{-1}. There was also some evidence that at temperatures below 1400°C the log D vs. 1/T plot showed a discontinuity with a lower activation energy occuring at low temperatures. This was not confirmed and no further work has been published. Anion self-diffusion was measured by Oishi and Kingery (1960) by determining the rate of exchange between a limited volume gas phase enriched with the stable isotope ^{18}O, and MgO grains. There appeared to be very little difference in coefficients for grain boundary and lattice diffusion. Values for D_o and Q were of the order of 10^{-6} cm^2 sec^{-1} and 2.7 eV respectively, over the temperature range 1300-1750°C. The oxide purity was about

99.9%. It was concluded that oxygen diffusion was either impurity-controlled or structure-sensitive under the conditions of the experiments.

Conductivity measurements (Mitoff, 1959, 1962, 1964) have led to somewhat confusing results. However, it now seems that MgO is predominantly an ionic conductor at temperatures around 1000°C and predominantly electronic above 1500°C. The ionic contribution decreases as the temperature is increased, the transport number falling from 0.88 at 1016°C to 0.33 at 1510°C. Application of the Nernst-Einstein equation to self-diffusion results indicates that the magnesium ion is the main carrier at low temperatures, since values of σ derived from Kingery's oxygen diffusion data are 10^3 times too small compared to the observed values. However, motion seems to proceed with a lower activation energy than that given by Lindner & Parfitt (1957), namely 2.17 eV as against 3.43 eV, a result which tends to confirm suspicions of the existence of a lower activation energy process for diffusion at low temperatures. At sufficiently high temperatures, Mitoff finds that all crystals show an activation energy of 3.5 eV. If in this region, MgO is an electronic conductor as Mitoff claims, this agreement with the activation energy for diffusion may be fortuitous.

1.2.2. Impurity Diffusion

Turning now to impurity diffusion, the first intensive study was carried out by Wuensch and Vasilos (1961, 1962,

1965). These workers have made a number of measurements of the diffusion of Fe^{2+}, Co^{2+}, Ni^{2+} and Zn^{2+} in single crystals of MgO. The temperature range covered was 1000-1700°C and the distribution of tracer after annealing was measured using electron microbeam probe spectroscopy. The diameter of the 30-KV electron beam was 1-2μ. However, in the course of later work (Wuensch and Vasilos, 1966a) it was found that, because of the light MgO matrix, fluorescence effects decrease the resolution of this technique to approximately 10μ. Diffusion couples were made both as "sandwiches" and by "vapour deposition", the most satisfactory method depending on the properties of the system concerned. The results of this work can be summarised by the following Arrhenius equations:-

$$\begin{aligned} Ni^{2+} &: D = 1.80 \times 10^{-5} \exp(-2.10/kT) \text{ cm}^2/\text{sec} \\ Co^{2+} &: D = 5.78 \times 10^{-5} \exp(-2.06/kT) \text{ cm}^2/\text{sec} \\ Fe^{2+} &: D = 8.83 \times 10^{-5} \exp(-1.81/kT) \text{ cm}^2/\text{sec} \\ Zn^{2+} &: D = 1.48 \times 10^{-5} \exp(-1.85/kT) \text{ cm}^2/\text{sec} \end{aligned} \quad \ldots\ldots \quad (1\text{-}15)$$

Rungis and Mortlock (1966) have recently published work on the diffusion of Ca^{2+} in MgO. They used an autoradiographic method to record diffusion profiles, over the same temperature range, and find values of Q and D_o of 2.13 eV and 2.95×10^{-5} $cm^2\ sec^{-1}$ respectively.

All the above results are characterised by low D_o values, but the authors (Wuensch and Vasilos, Rungis and Mortlock) considered them to apply to lattice diffusion, particularly when it was found that the activation energies could be correlated empirically to the ratio of the radius (r), of the diffusing cation to its electronic polarisability (α). This is simply expressed in the following equation

$$Q = k_1 \frac{r}{\alpha} + k_2 \qquad \ldots\ldots \quad (1\text{-}16)$$

where $k_1 = 0.37 \times 10^{16}$ eV.cm^2 and $k_2 = 1.20$ eV. A graph of Q vs. r/α is shown in fig 1.1. This correlation makes use of the Lindner and Parfitt value of 3.43 eV for the activation energy for cation self-diffusion, and has been regarded as applying to divalent ions diffusing in MgO by the same mechanism.

Brief mention should be made here of measurements of diffusion in polycrystalline MgO. Wuensch and Vasilos (1961) reported the grain-boundary diffusion of Ni^{2+} in MgO, and using a micrographic technique, Zaplatynsky (1962) noted similar results for Co^{2+} and repeated the Ni^{2+} study successfully. However, Shelly et al (1962) found no enhanced grain boundary diffusion for either Co^{2+} or Fe^{2+}. Further work by Wuensch and Vasilos (1964) confirmed their original findings, but this time Zaplatynsky (1964), again using a photomicrographic method, was unable to detect any enhanced diffusion of Co^{2+} and Ni^{2+}

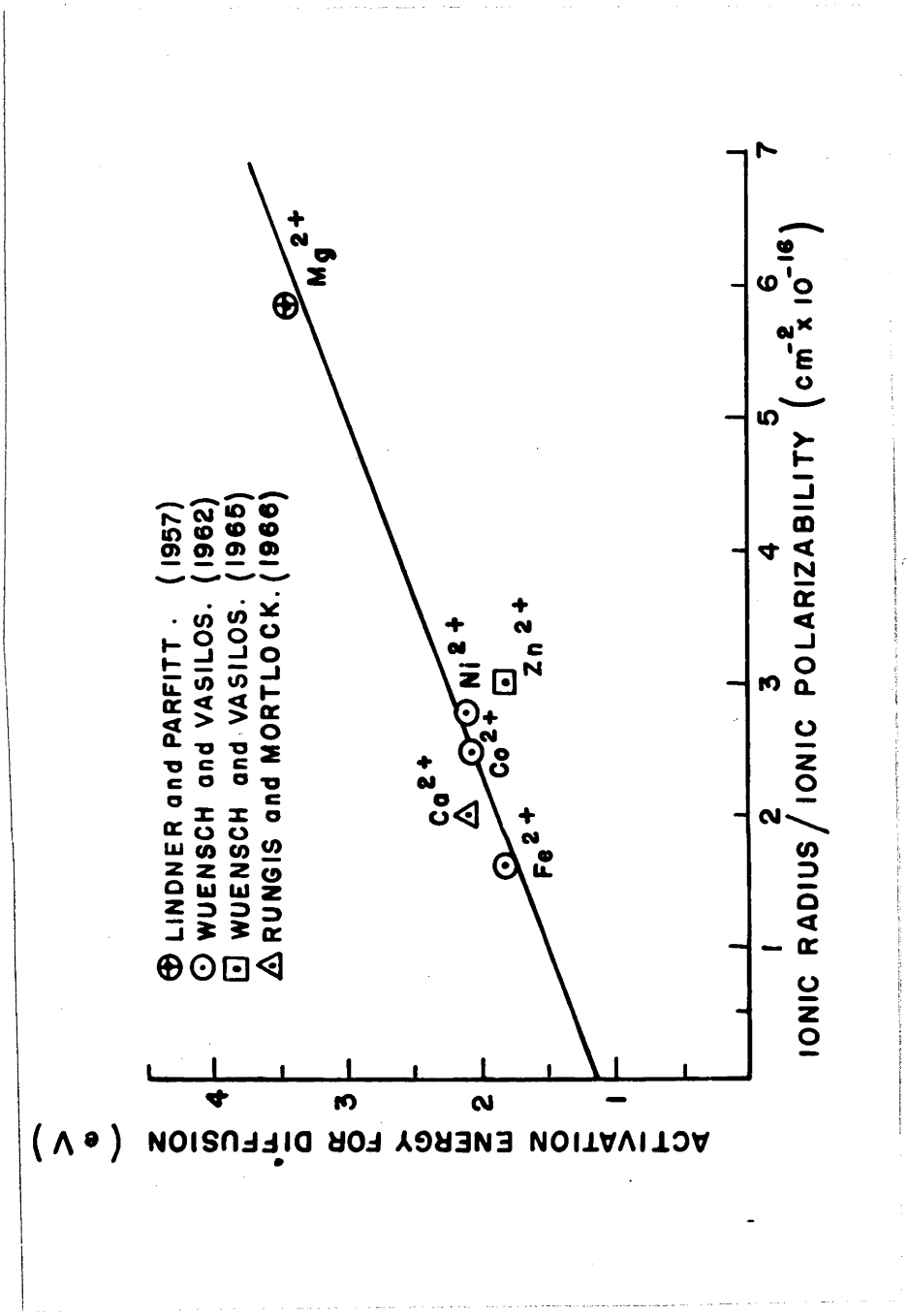

Fig 1.1 Correlation of activation energy for diffusion (Q eV) with the ratio ionic radius/ionic electronic polarisability (r/α).

along grain boundaries. No explanation of this contradiction was offered.

In an attempt to resolve this disagreement, recent work by Wuensch and Vasilos (1966b) has proved the preferential diffusion of Ni^{2+} and Co^{2+} along grain boundaries in MgO bicrystals, and indicates that this enhancement is due to impurity segregation at the boundary. The impurities responsible are Ca, Si and Fe. No enhancement has been observed in bicrystals prepared above 1300°C, at which temperature it is thought that impurity precipitates are re-absorbed into solid solution. Therefore enhanced grain boundary diffusion of cations in MgO is an extrinsic, rather than an intrinsic, property of the boundary and this could provide the explanation for the variety of results obtained by different workers.

One interesting aspect which Wuensch and Vasilos have found is that, unlike metal systems where the grain boundary width, δ, is only a few atomic spacings, in MgO it appears to be of the order of microns. In the work of Laurent and Benard (1955, 1958) grain boundary diffusion in alkali halides was clearly indicated but the concentration distribution of diffusant suggested that the kinetics of lattice diffusion applied. Wuensch and Vasilos (1964) suggested that extended grain boundaries in these crystals could explain this result.

It should be remarked at this point that grain

boundary diffusion usually leads to apparent values for D_o which are very low compared with those for lattice diffusion. Activation energies are also smaller. This is illustrated by the results for self-diffusion in silver (Hoffman and Turnbull 1951; Slifkin, Lazarus and Tomizuka, 1952)

$$\text{Polycrystal Ag:} \quad D = 2.3 \times 10^{-5} \exp(-1.14/kT) \text{ cm}^2/\text{sec}$$
$$\text{Single crystal Ag:} \quad D = 0.895 \exp(-1.99/kT) \text{ cm}^2/\text{sec} \qquad \ldots\ldots \quad (1\text{-}17)$$

The same relation between parameters is found for dislocation influenced diffusion. Indeed, grain boundaries can be described by a dislocation model under certain conditions (e.g. Girifalco, 1964 p.124). Keeping this in mind, it is interesting to note that diffusion in some polycrystalline ionic solids is described by parameters similar to those which appear to apply to single crystal material. In addition to the results for oxygen diffusion in MgO already quoted, Ni diffusion in NiO (Shim and Moore, 1957) provides an example of this:-

$$\text{Polycrystal NiO:} \quad D = 5.0 \times 10^{-4} \exp(-1.91/kT) \text{ cm}^2/\text{sec}$$
$$\text{Single crystal NiO:} \quad D = 3.9 \times 10^{-4} \exp(-1.91/kT) \text{ cm}^2/\text{sec} \qquad \ldots\ldots \quad (1\text{-}18)$$

During the course of their study of grain boundary diffusion in MgO, Wuensch and Vasilos (1966a) repeated the measurement of Ca^{2+} diffusion in single crystal MgO over the

same temperature range as that studied by Rungis and Mortlock. They have quoted only tentative results as yet, but they do not agree with those previously obtained. The activation energy is reported to be 3.3 eV and the pre-exponential factor is 0.025 cm^2 sec^{-1}. These figures do not agree with the correlation, equation (1-16), but no comment was made on this.

1.3. Aim of the Present Study

The aim of the present work is to test equation (1-16) to its limits, and the two impurities selected, Be (Harding and Mortlock, 1966) and Ba (Harding, 1967), have values of r/α (Pauling, 1960; Mott and Gurney, 1940) which lead to predicted activation energies of 15.7 eV and 1.53 eV respectively. The former is unreasonably high, but the latter is within the realms of possibility although it would appear to be rather low for such a large ion. However, past work has indicated that the polarisability, α, plays an important part in determining activation energies. A relationship such as equation (1-16) could be the first step in understanding oxide systems in general, but as a result of the work described in this thesis, another explanation will be advanced for the diffusion parameters observed in experiments on MgO.

II. THEORY AND GENERAL METHOD

2.1. Solutions to the Diffusion Equation

In experimental methods usually used to measure diffusion in solids, a thin deposit of impurity is placed on the surface of the solvent concerned and during annealings at a temperature T for a period of t seconds, this impurity containing radio-active tracer atoms, diffuses into the host lattice. The starting point for determining the theoretical distribution of the impurity after annealing, is Fick's Second Law of Diffusion (e.g. Shewmon, 1963 p.5). Considering diffusion in the x direction only, we have -

$$\frac{\partial C}{\partial t} = \frac{\partial}{\partial x}\left(D \frac{\partial C}{\partial x}\right) \qquad \ldots\ldots \quad (2\text{-}1)$$

If D (the diffusion coefficient) is not a function of the concentration C, this equation reduces to

$$\frac{\partial C}{\partial t} = D \cdot \frac{\partial^2 C}{\partial x^2} \qquad \ldots\ldots \quad (2\text{-}2)$$

There are two sets of boundary conditions which must be considered in solving this equation for C. For a thin surface source diffusing in the x direction, the set of conditions can be written

$$\text{For } x > 0,\ C \longrightarrow 0 \text{ as } t \longrightarrow 0$$

$$\text{and for } x = 0,\ C \longrightarrow \infty \text{ as } t \longrightarrow 0$$

The solution to equation (2-2) is then

$$C = \frac{M}{2\sqrt{\pi D t}} \cdot \exp\left(-x^2/4Dt\right) \qquad \ldots\ldots \quad (2\text{-}3)$$

where M is the total amount of tracer-bearing impurity deposited on the surface. This may be referred to as the "Gaussian solution". Since the pre-exponential term can be assumed constant for a given annealing time, the impurity distribution is such that a plot of ln C vs. x^2 will yield a straight line of slope $-1/4Dt$. The deposited layer must be thin, that is, negligible in comparison with $\sqrt{Dt}$, because it has been assumed that the whole deposit M, can take part in diffusion - that is, the quantity of surface material deposited must go into solution in a time that is short compared with the annealing time, often arbitrarily set at 0.01 t.

If the solubility is small or the deposited layer thick, the above conditions are no longer applicable. The only impurity taking part in diffusion is that in solution at any particular moment and as the solute diffuses into the solvent, further quantities of the deposit can go into solution at the surface. If the surface concentration does not fall below the solubility limit at all during annealing, the appropriate boundary conditions are given by

$$C = 0 \text{ at } t = 0 \text{ for } 0 < x < \infty$$

$$\text{and } C = C_s \text{ at } x = x_s \text{ for } 0 < t < \infty$$

and the solution to equation (2-2) is

$$C = C_s \operatorname{erfc} \frac{x - x_s}{2\sqrt{Dt}} \qquad \ldots\ldots \quad (2\text{-}4)$$

where C_s is the solubility limit of the primary phase and x_s is the thickness of the zone of surface phases where the solute concentration is greater than C_s. The application of this solution, which can be referred to as the "error function solution", assumes that x_s is independent of time. In many cases, it is small compared with the penetration x and can be assumed to be zero. Experimental difficulties sometimes encountered in the application of this solution have been treated by Mortlock (1964) and are briefly described in paragraph 2.2.2.

The minimum surface deposit required for the error function solution to apply can be calculated as follows. The total amount of impurity which has gone into solution during an annealing of duration t is given by

$$S = \int_0^\infty C_s \operatorname{erfc} \frac{x}{2\sqrt{Dt}} \cdot dx \qquad \ldots\ldots \quad (2\text{-}5)$$

If M is the amount deposited, it must be greater than S.

Putting $u = \frac{x}{2\sqrt{Dt}}$ we have

$$S = 2\, C_s . \sqrt{Dt} \int_0^\infty \operatorname{erfc} u . du \qquad \ldots\ldots \quad (2\text{-}6)$$

Now, $\int \operatorname{erfc}.(x)dx = x.\operatorname{erf}(x) + \frac{1}{\sqrt{\pi}} \exp(-x^2)$

and $\operatorname{erfc}.(x) = 1 - \operatorname{erf}(x)$

Applying these two identities, the integral in equation (2-6) can be evaluated and we arrive at

$$S = 2 C_s \cdot \sqrt{\frac{Dt}{\pi}} \qquad \ldots\ldots \quad (2\text{-}7)$$

With a knowledge of the solubility of the impurity in MgO (e.g. Levine, Robbins and McMurdie, 1964) S can be calculated for a given value of $\sqrt{Dt}$ and compared with M, which is obtainable from the specific activity of the tracer solution used. In some cases C_s is not known, but under certain circumstances S can be measured directly. This situation occurred in the case of barium diffusing in MgO, and will be considered later.

2.2. Radioactive Tracer Techniques

2.2.1. General Comments

The use of radioactive isotopes is a convenient method of studying diffusion in solids, and it has been used extensively for many years. The variety of tracer materials available increased rapidly with the expansion of reactor technology. In addition to the techniques to be described in this work, a number of absorption techniques have been described (Cadek and Janda, 1957, 1959). Even though the ratio of the diffusion coefficients for different isotopes of the same chemical species can be as great as the ratio of the square roots of their mass numbers, (Mullen, 1961) this variation is usually well within the limits of precision to which measurements can be made. Thus it is permissible to take the diffusion coefficients found using isotopes as applicable to other atoms of the same element. In recent years, however,

experiment has indicated that this "isotope effect" can be a useful tool in the determination of correlation factors (Barr and Le Claire, 1964; Barr and Mundy, 1965; Le Claire, 1966) and hence can sometimes give an indication of the diffusion mechanism operating in a particular system. The problem of measuring D to the necessary precision can be overcome by diffusing the two isotopes concerned simultaneously.

Some advantages of the technique are that the impurity can be easily detected using Geiger-Muller or scintillation counting, or autoradiography, and these methods are extremely sensitive allowing studies to be made at near-zero concentrations. Also, each isotope has a characteristic radiation so that it can be followed without ambiguity. Certain properties are required if an isotope is to be useful in diffusion work. These can be listed briefly as follows:-

(a) its half-life should be sufficiently long because annealing can take several weeks, or even months, to complete, in particular where measurements are made at low temperatures, (that is, for T less than half the melting point temperature); and

(b) its specific activity should be as high as possible, so that small quantities can be detected easily and a sufficiently large number of counts can be obtained to minimise statistical errors.

The method used in any given case for following the diffusing tracer depends on the system being studied, and the tracer used. Autoradiography requires a tracer with "soft" radiation which is easily stopped by photographic emulsions in order to obtain satisfactory resolution of the profile image. Sectioning techniques are best employed when radiations involved are "hard". For intermediate and low values of the absorption coefficient of the radiation in the material studied, the "surface activity decrease" method can be applied. In this case, the volatility of the tracer material must be very low at the temperatures concerned. Autoradiography has the advantage that individual coefficients for different regions of the same crystal can be measured, whereas serial sectioning in addition to being destructive, yields only an average coefficient for the whole crystal. This advantage, however, tends to be partly cancelled by possible errors arising from the analysis of the autoradiographic image. The extent of these errors depends on the isotope employed. The following paragraphs describe in more detail the application of the above theory to the systems examined in this project.

2.2.2. Calcium Diffusion

The tracer used in this case, ^{45}Ca, is suitable for the application of autoradiography. The radiation, 0.25 MeV β^-, is soft and therefore has a short range in MgO and in the

photographic emulsion used. If the diffusion couple is suitably sectioned and X-ray film placed in contact with it, then each point along the penetration profile gives a corresponding point image on the film, under ideal conditions. In practice, a "resolution" correction has to be applied. A full treatment of this correction is described elsewhere (Rungis and Mortlock, 1966; Brown and Blackburn, 1963). Briefly, an undiffused "sandwich" does not give a line image on the film and an apparent value of the product Dt can be derived by assuming that the density of the image obtained has a distribution described by the Gaussian solution to the diffusion equation. For the appropriate annealing time t, a correction can be calculated which is subtracted from the apparent diffusion coefficients obtained from annealed couples.

For an annealed couple, a concentration vs. penetration curve is derived from the intensity of the photographic image in the following manner. Using a microdensitometer, the image is scanned and the variation of density with distance perpendicular to the diffusion interface is traced on a chart recorder. The concentration of diffusant at a given penetration x is then proportional to $\log (I_o/I_x)$, where I_o is the intensity of light transmitted through the unexposed part of the film and I_x is that transmitted through the exposed part at a distance x along the profile from the diffusion

interface, provided that log (I_o/I_x) does not exceed a value which is characteristic of the film employed.

The error function solution, equation (2-4), applies to Ca diffusion in MgO due to the small solubility of CaO in MgO. Rewriting equation (2-4) as

$$(\text{erfc})^{-1} \frac{C}{C_s} = \frac{x}{2\sqrt{Dt}}$$

and provided C_s can be obtained by extrapolating the profile back to x = 0, a plot of $(\text{erfc})^{-1} \frac{C}{C_s}$ vs. x will yield a straight line the slope of which gives D, the apparent diffusion coefficient. From this, the resolution correction is subtracted to give the true diffusion coefficient.

However, sometimes it is not possible to derive C_s by extrapolation with sufficient accuracy and in this event the following analysis (Mortlock, 1964; Rungis and Mortlock, 1966) can be used. If a plot is made of ln C vs x^2, a curve results, but a straight line can be fitted to this curve over a limited range of x^2 and an apparent diffusion coefficient D_a can be found from its slope as if the Gaussian solution applied. D_a is related to the correct value of D, (D_c) which operates in equation (2-4) by:-

$$\frac{D_c}{D_a} = \sqrt{\frac{D_c t}{\pi}} \cdot \frac{2 \exp(-x^2/4D_c t)}{x.\text{erfc}\ (x/2\sqrt{D_c t})} \qquad \ldots\ldots \quad (2\text{-}8)$$

This indicates that D_c/D_a is constant providing D_a is

evaluated at the same effective value of $x^2/D_c t$ in each experiment. The proportionality factor is best evaluated empirically by comparing the values of D_a and D_c calculated separately in a run in which the data is sufficiently smooth that not only equation (2-3) may be used to evaluate D_a but also the differential of equation (2-4) to yield D_c. In this way, the need to know the solubility of the diffusant in the MgO is eliminated.

2.2.3. Beryllium Diffusion

For a study of the impurity diffusion of Be in MgO, the most convenient method to use is that of sectioning, because the tracer available, ^{7}Be, emits a γ ray of energy 0.48 MeV. It is not easy experimentally however to determine the concentration vs. penetration distance profile directly since the sections removed are very thin and the count rate obtained from them very small. There is also the problem of collecting the material removed. It is better therefore, to measure the activity remaining in the bulk of the crystal after the removal of each section. This leads to an integrated profile. At any depth x' from the original surface, we can write for the activity remaining

$$A(x') = \int_{x'}^{\infty} C(x)\, dx \qquad \ldots\ldots \quad (2\text{-}9)$$

This is valid for a given annealing time t when the constant of proportionality between count rate and concentration has

been omitted. At $x' = 0$, we have:-

$$A(0) = \int_0^\infty C(x)\, dx \qquad \ldots\ldots \quad (2\text{-}10)$$

The "fractional activity remaining" $F(x')$ is then given by

$$F(x') = \frac{A(x')}{A(0)} = \frac{\int_{x'}^\infty C(x)\, dx}{\int_0^\infty C(x)\, dx} \qquad \ldots\ldots \quad (2\text{-}11)$$

For BeO, it was found that the solubility in MgO is high from the point of view of diffusion, being of the order of 2 mole % at 1000°C and increasing with temperature (Levine, Robbins and McMurdie, 1964). The "Gaussian solution" to the diffusion equation is therefore applicable and substituting for $C(x)$ gives

$$F(x') = \frac{\int_{x'}^\infty \exp\,(-x^2/4Dt)\, dx\ .}{\int_0^\infty \exp\,(-x^2/4Dt)\, dx} \qquad \ldots\ldots \quad (2\text{-}12)$$

Now the denominator is a standard integral of the form

$$\int_0^\infty \exp(-a^2 x^2)\, dx = \frac{1}{2a} \cdot \sqrt{\pi} \qquad \ldots\ldots \quad (2\text{-}13)$$

Using this identity in equation (2-12) gives

$$F(x') = \frac{2}{\sqrt{\pi}} \int_{x'}^\infty \exp\,(-\frac{x^2}{4Dt}) \cdot \frac{dx}{2\sqrt{Dt}} \qquad \ldots\ldots \quad (2\text{-}14)$$

Making a change of variable and putting $u = \frac{x}{2\sqrt{Dt}}$ we arrive at

$$F(x') = \frac{2}{\sqrt{\pi}} \int_{u'}^\infty e^{-u^2}\, du \qquad \ldots\ldots \quad (2\text{-}15)$$

This equation can be written using standard notation for the error function complement as

$$F(x) = \text{erfc}\ (u) \qquad \ldots\ldots \quad (2\text{-}16)$$

Thus if the fractions F(x) are measured for various values of x, then the corresponding values of u, the limit of the integral in equation (2-15), can be obtained from mathematical tables (e.g. Carslaw and Jaeger, 1959).

In effect, plotting $(\text{erfc})^{-1}\ F(x)$ against x gives a straight line of slope $\frac{1}{2\sqrt{Dt}}$ from which D can be calculated.

2.2.4. Barium Diffusion

A similar calculation to that carried out above can be performed in this case. The tracer used was ^{133}Ba and the same techniques were employed as in the study of Be diffusion in MgO. In this work, however, the experimental profiles always showed the presence of excess undissolved tracer on the surface of the crystal being sectioned. This indicated that the solubility of BaO in MgO is very small and the "error function solution" to the diffusion equation is applicable to this system. Substituting equation (2-4) into equation (2-11) and assuming x_s is essentially zero gives

$$F(x') = \frac{A(x')}{A(0)} = \frac{\int_{x'}^{\infty} \text{erfc}\ \left(\frac{x}{2\sqrt{Dt}}\right)\ dx}{\int_{0}^{\infty} \text{erfc}\left(\frac{x}{2\sqrt{Dt}}\right)\ dx} \qquad \ldots\ldots \quad (2\text{-}17)$$

It must be pointed out that A(0) is not the initial activity recorded from the crystal before sectioning begins as was the case for Be. A(0) here is the point where the extrapolated experimental plot of A(x) vs. x cuts the x = 0 axis, and represents the count rate from the total amount of material in solid solution after the annealing of the couple. Putting $u = \frac{x}{2\sqrt{Dt}}$ again and evaluating the denominator from a standard integral leads to the equation

$$F(x') = 1.772 \int_{u'}^{\infty} \text{erfc.}(u)\, du \quad \ldots\ldots \quad (2\text{-}18)$$

Using the notation, $\text{ierfc}(a) = \int_{a}^{\infty} \text{erfc}\, y\, dy$ we can write

$$F(x) = 1.772 \cdot \text{ierfc}(u) \quad \ldots\ldots \quad (2\text{-}19)$$

Again, for several measurements of F(x) we can plot a graph of $(\text{ierfc})^{-1}\, F(x)$ against the penetration (x) and obtain a straight line, the slope of which is $\frac{1}{2\sqrt{Dt}}$. From this D can be calculated as before.

In both the analyses in the above paragraphs, the absorption of the radiations in MgO has been assumed to be negligible. This assumption has been shown to be justified and absorption measurements are described in the next chapter.

III. APPARATUS AND MATERIALS

3.1. Magnesium Oxide Single Crystals

3.1.1. General Properties

The single crystals used in this study were supplied by the Monocrystals Company, Cleveland, Ohio, U.S.A., in the form of right cylinders, $\frac{1}{4}$" in diameter and $\frac{1}{4}$" in length. They were supplied cut such that a [100] plane was perpendicular to the cylinder axis and could therefore be easily cleaved to form two cylinders of approximately equal size. MgO consists of two face-centred cubic sub-lattices and this structure is shown diagrammatically in Fig 3.1. Other physical properties are set out in Table (3.1).

3.1.2. Impurities

The rates of diffusion in ionic solids have been shown to be strongly dependent on impurity content, due to the need to maintain electrical neutrality in the lattice (see Introduction). The main impurities in MgO are Ca, Fe and Al. Ca should have no effect on measured diffusion coefficients but Al and Fe could be of importance. To preserve the required electrical neutrality, every two trivalent ions present on Mg^{2+} sites would give rise to a cation vacancy. This would lead to an extrinsic region for which the activation energy is lower than would be expected for intrinsic lattice diffusion as was discussed in relation to the alkali

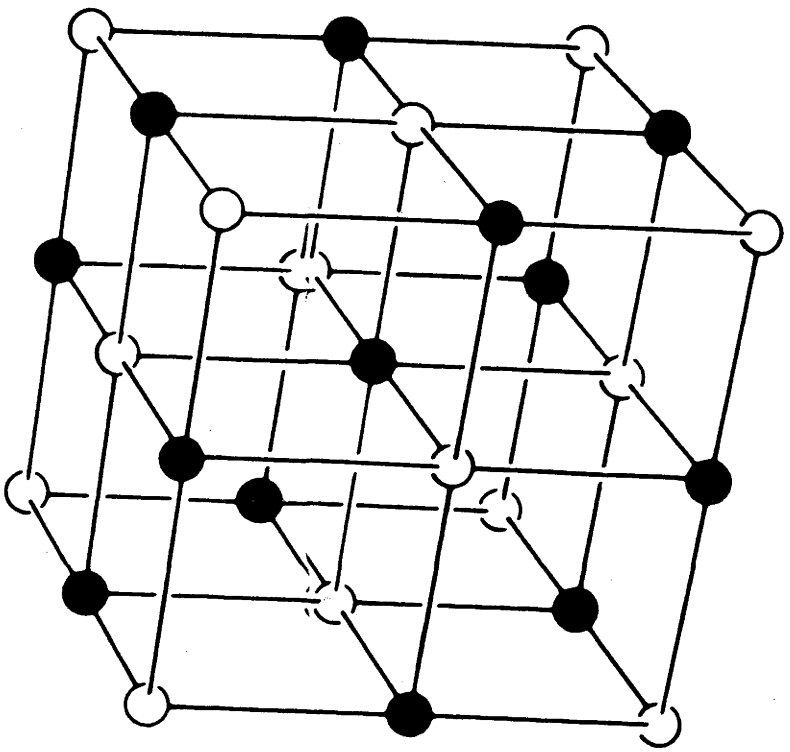

Fig 3.1 The crystal structure of MgO.

TABLE 3.1

Property	Value
Molecular weight	40.32
Density	3.65 gm cm^{-3}
Refractive index	1.736
Colour	Colourless and transparent
M.p.	2800°C
Coefficient of expansion (linear)	13.5 x 10^{-6} $^{o}C^{-1}$
Hardness (Moh's scale)	6.0
Thermal conductivity	0.014 c.g.s. units at 1100°C
Specific heat (28-1000°C)	0.28 cal/gm/°C
Crystal structure	f.c.c. (NaCl type)
Cleavage	<100>
Lattice constant a_o	2.1 Å

halides. In order to reduce the effects of these trivalent ions, the highest purity crystals available were used in this work. The present source of supply seems to be superior to any previously cited in the literature and details of the levels of various impurities present are shown in Table 3.2. The overall purity claimed by the supplier is 99.99% and this appears to have been confirmed qualitatively by the Defence Standards Laboratory, (D.S.L.), Melbourne. Only the major impurity elements are quoted here. Several others whose presence may have been suspected, were not detected.

3.1.3. Crystallographic Defects

Another factor which can greatly influence diffusion in single crystals is the defect concentration. In addition to Schottky and Frenkel defects giving rise to anion and cation vacancies and interstitials ("point defects"), other more extensive disorder occurs.

A "dislocation" is formed when one part of a perfect lattice is displaced relative to an adjacent part. At the dislocation core, the atomic misfit can be quite large and the resulting disorder and looseness can greatly enhance diffusion in this region. In addition to this "pipe" diffusion, another effect operates in ionic solids. It has been found that in magnesium oxide, dislocations are positively charged (Rueda and Dekeyser, 1961) and therefore there must be a

TABLE 3.2

Impurity	Analysis (p.p.m.)	
	Monocrystals	D.S.L.
Ca	10	Trace
Fe	25	Faint trace
Al	25	Faint trace
Si	10	Not detected
Pb	10	Trace
In	15	Not detected
Others, total	<30	-

correspondingly large concentration of cation vacancies in the region of the dislocation line. It can therefore be said that if these features exist in any great numbers, the parameters for diffusion in magnesium oxide will be markedly affected. In an attempt to detect their existence in the crystals used in this study, a number of photomicrographs were taken of MgO surfaces in the expectation that impurity precipitates decorating these features would indicate an order of magnitude figure for the dislocation density.

Four MgO crystals were selected for a photomicrographic study. Two were embedded in normal (i.e. inactive) BaO powder in an alumina crucible and heated at 1240°C for a period of 48 hours. These crystals were then cleaved perpendicularly to the cylinder axis to expose [100] surfaces. These surfaces were examined using a Vickers Projection Microscope capable of magnifications of up to 4500 X. These and two other crystals selected later from those used in diffusion experiments were subsequently mounted in metallurgical mounting plastic, and polished firstly with diamond paste down to 1μ grade, then with α-alumina (particle size 0.3μ). The surfaces thus produced were etched using 1:1 hydrochloric acid or concentrated nitric acid. A number of photomicrographs were then taken.

Examples of surface steps on the cleaved surfaces of

the crystals are shown in Figs 3.2, 3.3. It has been suggested that these steps start at points where dislocations cut the exposed surface and converge into larger steps which build up characteristic river patterns (Fiedel, 1964). Numerous large steps are also produced by plastic straining and these "slip lines" have Burgers vectors which can reach thousands of Angstroms. At a much higher magnification, the photomicrographs obtained are shown in Figs 3.4, 3.5. These show rows of pyramid-like structures near the surface of a cleaved crystal. Bowen and Clarke (1963) found similar structures in MgO and suggested that they are associated with impurity precipitates along dislocations. In view of the work of Venables (1963) who was able to identify ZrO_2 precipitates and use them to estimate a diffusion coefficient for Zr in MgO, it would seem reasonable to suggest that the pyramids in the present work are indeed associated with barium oxide precipitates. The density of the pyramids was comparable with that found by Bowen and Clarke, namely $10^5 - 10^7$ cm^{-2}. The fact that they show up on a cleaved surface can be explained by the presence of a stress field causing the lattice to crack around, rather than through, the precipitates. The average distance between the rows of pyramids is 3.5μ. This agrees with the value of 2-5μ for the mean distance between dislocations found by Lang and Miles (1965) in an X-ray topographic study of MgO crystals.

The dislocation density then, for the crystals to be

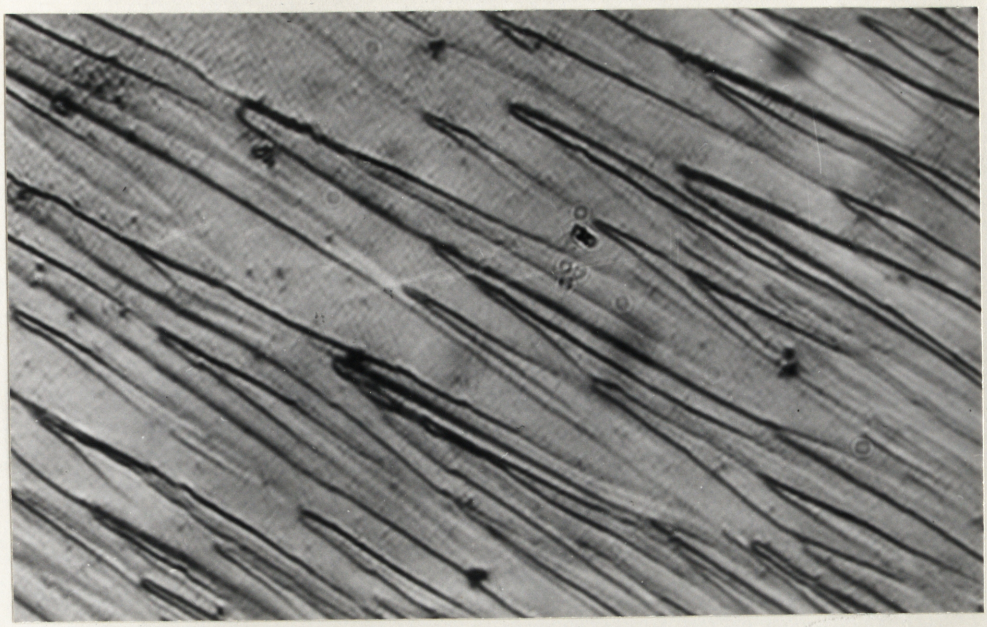

Fig 3.2 Steps on a cleaved MgO surface (X 570)

Fig 3.3 Steps on a cleaved MgO surface (X 100)

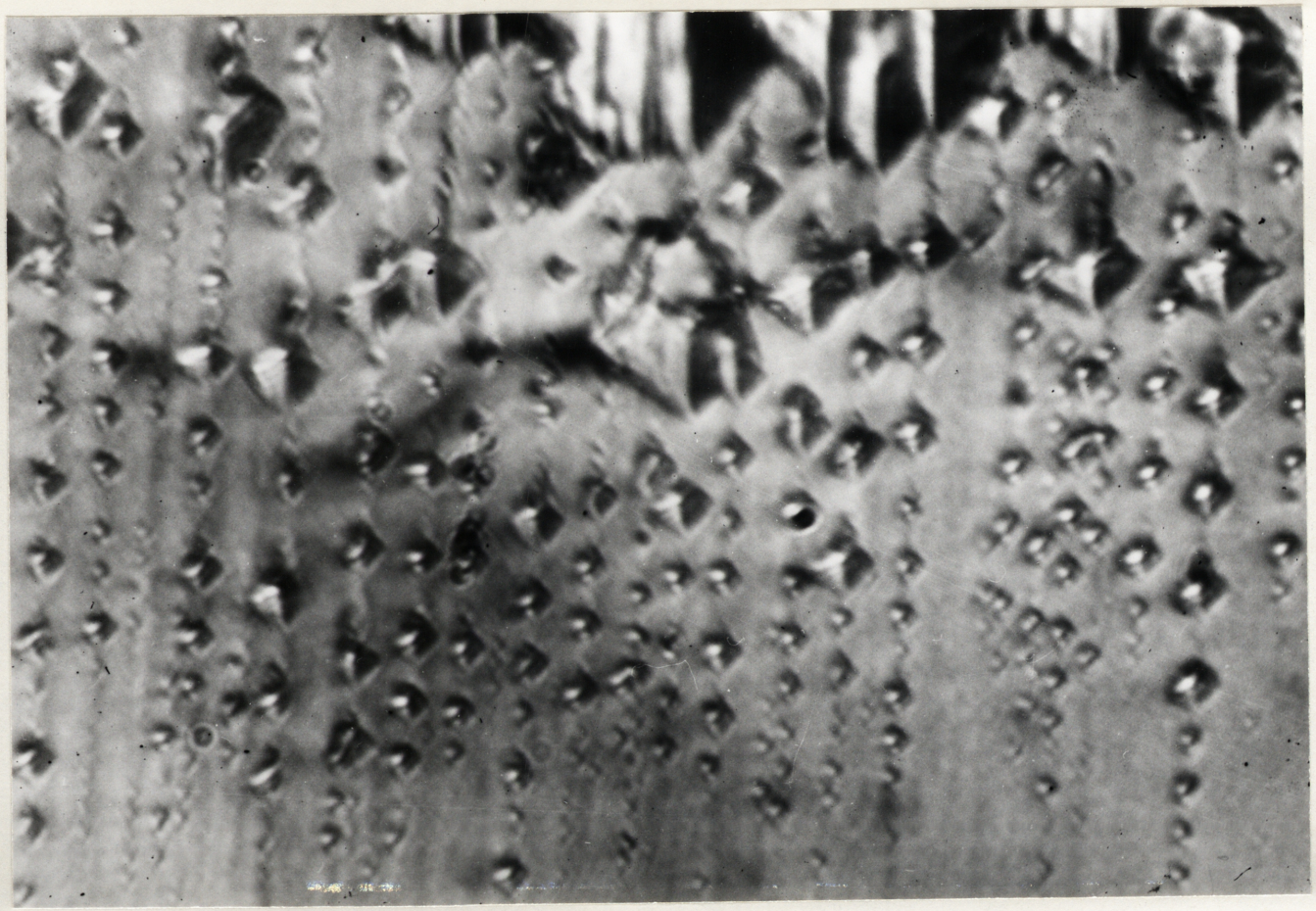

Fig 3.4 Pyramid structures near the edge of a cleaved MgO surface (X 2000)

Fig 3.5 Pyramid structures near the edge of a cleaved MgO surface (X 2000)

studied here can be said to be of the order of 10^7 cm^{-2}. It will be seen later that a density of this magnitude strongly influences measured diffusion coefficients.

3.2. Radioisotopes Used

All the isotopes used were supplied by the Radiochemical Centre, Amersham, England. As mentioned previously, ^{45}Ca emits a β^- particle of 0.25 MeV and has no other radiations. Its half-life is 164 days, and it was obtained as chloride in solution with a specific activity of 2.5 curie per gm of Ca.

For the experiments on beryllium diffusion in MgO, ^7Be was employed. This tracer emits a γ ray at 0.48 MeV and soft X-rays. It was supplied "carrier free" in dilute HCl solution with an initial activity of 1 mc. Its half-life is 53 d. ^{133}Ba has several γ peaks in its spectrum with the strongest at 0.358 MeV. The half-life of this isotope is 10 years and its specific activity as supplied was 1.6 curie per gram of Ba in HCl solution.

The equipment used for counting included an ECKO type N664 A preamplifier with a 13 dynode E.M.I. photomultiplier tube, and a 1" thallium-activated sodium iodide crystal was used as a scintillator. The settings of the gain, and window width of the amplifier/analyser were those which gave an optimum for the count rate to background ratio with 750

volt H.T. on the photomultiplier. The γ peaks of interest here for ^{7}Be and ^{133}Ba were identified using several standard sources available in the laboratory, and the calibration of threshold volts against γ energy is plotted in fig 3.6. The commercially supplied "castle" enabled a geometry to be used which could be reproduced accurately for every count. Fig 3.7 shows the absorption of the γ rays of both isotopes in magnesium oxide. Log (I_x/I_o) is plotted against the thickness of MgO traversed, where I_o is the γ ray count for no absorber and I_x is the count with MgO thickness x interposed between the source and detector. It can be seen that over the diffusion distances involved, practically no error was introduced by assuming zero absorption.

3.3. Furnaces and Temperature Measurement

Platinum-rhodium wound resistance furnaces were used for annealing diffusion couples. One was controlled by a Cambridge 5" two-step indicator-controller using a Pt-Pt/10% Rh thermocouple. A second, manufactured by A.D.A.M.E.L. Paris, was controlled mechanically by the expansion of the ceramic former on which the element wire was wound. This proved very satisfactory for operation up to 1400°C but the life of the element itself was rather short. For temperatures up to 1700°C, a vertical Johnson-Matthey furnace (type TK2) was used and it was controlled by a Leeds and Northrop

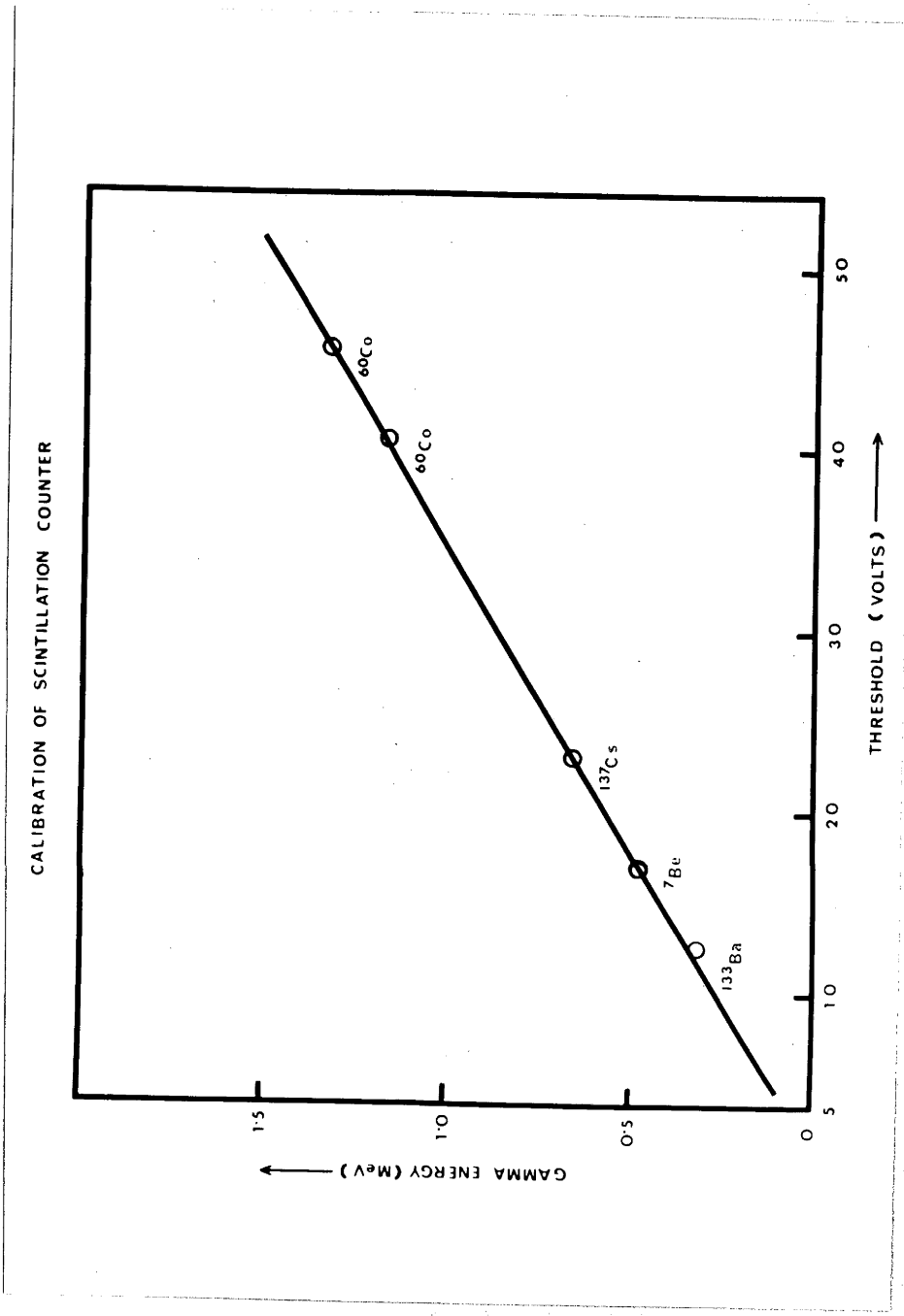

Fig 3.6 Calibration of scintillation counter and identification of the γ ray peaks of tracers used

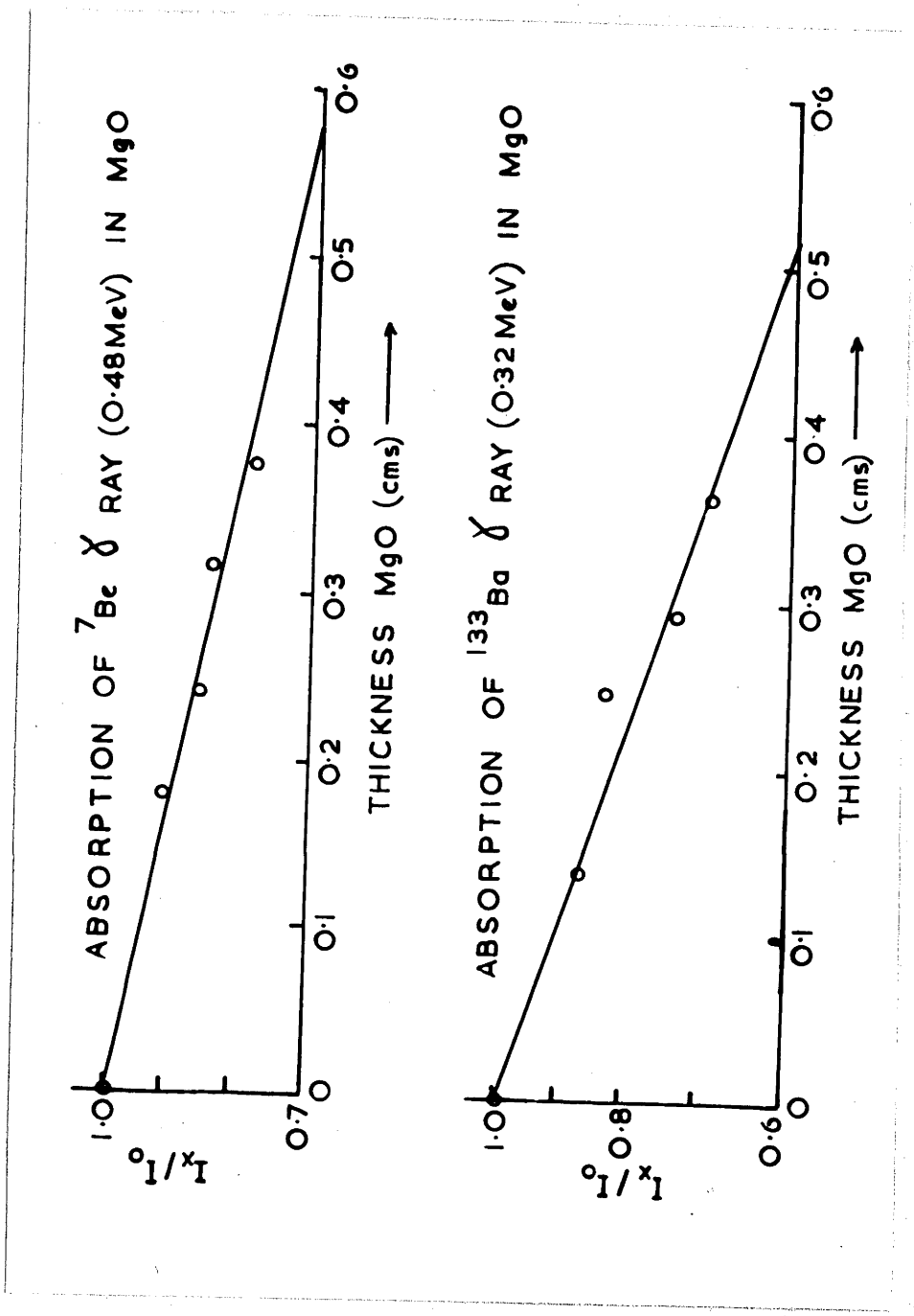

Fig 3.7 Absorption of ^{7}Be and ^{133}Ba γ rays in MgO.

"Rayotube" total radiation pyrometer coupled to a Leeds and Northrup "H" type controller-recorder. The furnace gave excellent service and element life was of the order of twelve months with fairly frequent usage.

Temperatures were measured, independently of the furnace control units, with a Leeds and Northrup potentiometer type K-3 and Pt-Pt/10% Rh thermocouples up to 1500°C, and a Pt-Pt/18% Rh couple for readings up to 1700°C. A continuous record was also kept using a multichannel recorder (Leeds and Northrup type W). Sunvic CJ1 electric cold junctions were employed to eliminate the effects of ambient temperature variations. All thermocouples and the potentiometer were calibrated by the National Standards Laboratory, Sydney. The accuracies quoted were generally 0.2% for the thermocouples and 0.01% for the potentiometer readings. This, of course, is not the accuracy to which the temperature for the total diffusion run can be measured and this will be discussed later, along with other sources of error.

Before any annealing was carried out, the temperature gradients in the furnaces were checked. The length of the hot zone in the furnaces over which the temperature could be regarded as uniform was limited. A typical limit at 1400°C was ± 5°C over a length of 2". Over the dimensions of the diffusion couples ($\frac{1}{4}$") the gradient was negligible. The

measured temperature with a thermocouple in contact with the diffusion couples could be regarded as being the same as that at the diffusion interface to well within the limits of control.

3.4. Precision Grinders

Many precision grinders have been described in the literature, some being very complex instruments (e.g. Leblans and Verheijke, 1963/64; Letaw, Slifkin and Portnoy, 1954). In this work it was found that the simplest design possible gave satisfactory results. For the studies with beryllium, a grinder described by de Bruin and Clark (1964) was used. This is shown in fig 3.8. However it was found that the micrometer scale on the body of the instrument was not very practicable as it was difficult to detect at which point grinding of the crystal surface actually began. A comparator was therefore used to measure section thicknesses (Starrett, model 25-511). The grinder itself slides on short "rails", the upper surfaces of which had been machined flat and aligned parallel to 1μ. In the trough between the rails was fixed a strip of 600 grit carborundum paper supported with a piece of plate glass. This method of removing layers from the sample, mounted in a nylon collet which could be attached to the grinder with a screw collar, proved adequate for measuring Be diffusion as the penetrations involved were

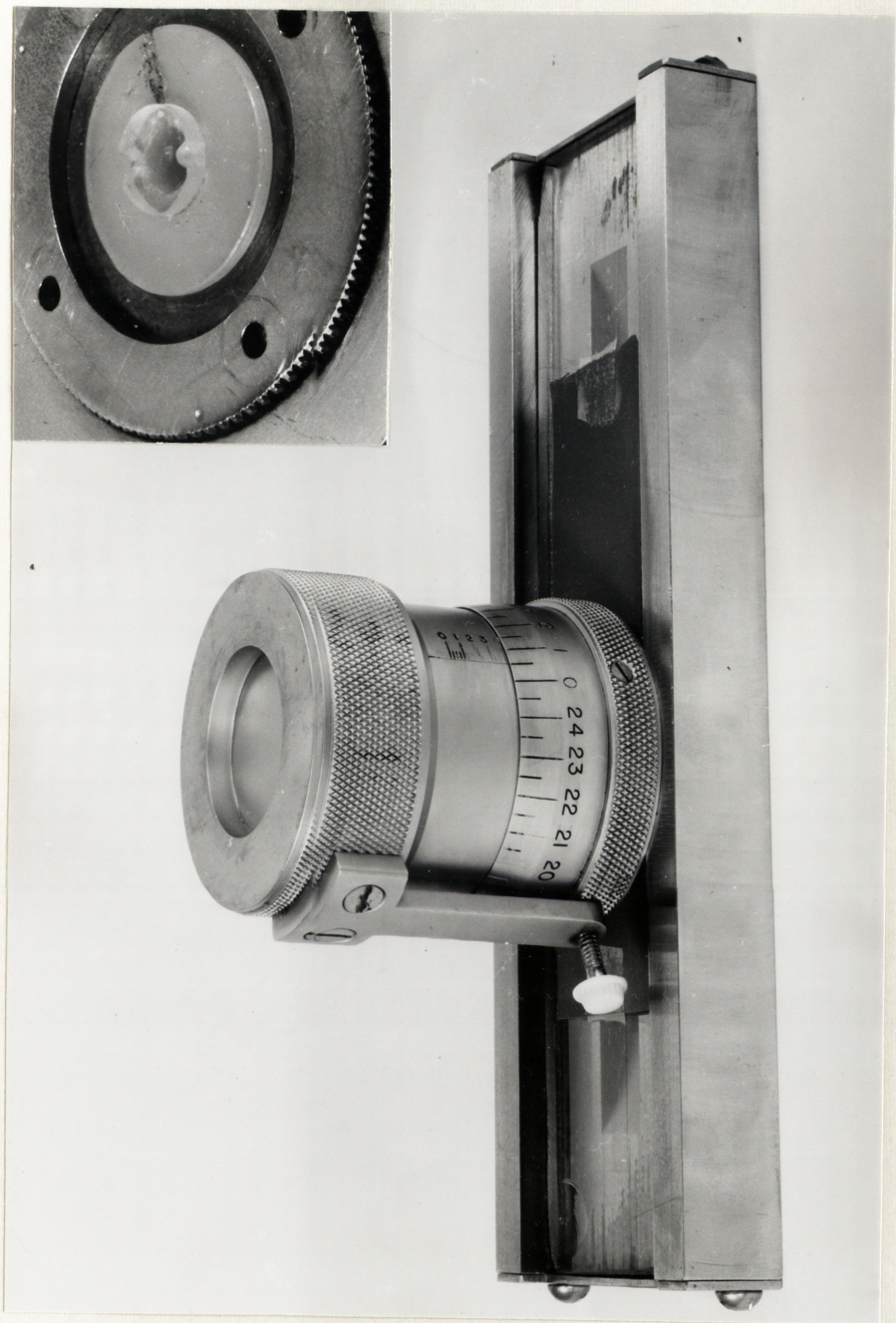

Fig 3.8 Precision grinder used in ^{7}Be diffusion study

commonly in the 100-200μ range. Sections could be taken as thin as 5μ. The disadvantage of using carborundum paper for grinding is that it gives rise to "crowning". This is illustrated in fig 3.9. The initial diffusion surface is essentially flat (cleavage was used to divide the as-received crystals here) but the surface produced by grinding was found to be very slightly convex. The distance B'P was measured and found to be about 3μ. The measured penetration distances were obtained from a mean of several comparator readings, one or two from the centre of the surface and up to ten around the

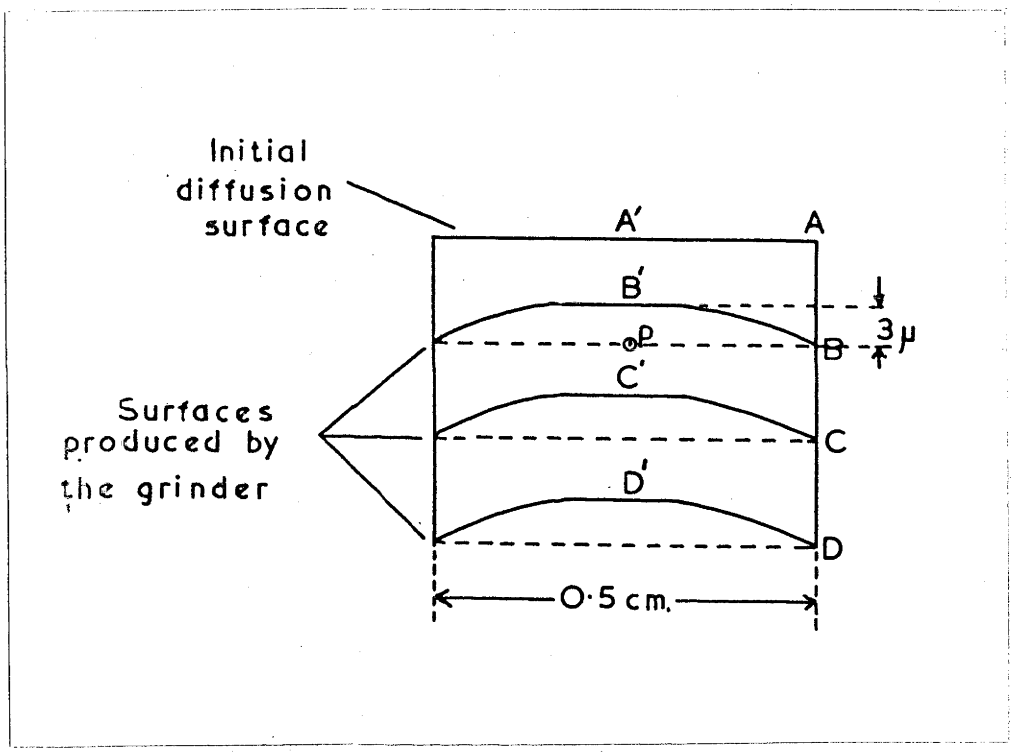

Fig 3.9 "Crowning" of a crystal during sectioning (vertical scale greatly exaggerated)

perimeter region. The mean was therefore biased towards AB as the penetration distance corresponding to the first count of the tracer remaining, A(x), instead of A'B'. Subsequent sectioning using the same method of measurement introduced no further error since B'C' is equal to BC and so on. The effect of this on the results will be referred to later.

For the analysis of Ba diffusion profiles, the above instrument was not suitable because the penetrations involved here were normally between 10μ and 20μ. For low temperatures, $\sqrt{Dt}$ was less than 3μ. The grinder shown in fig 3.10 was used for these experiments. It consists of an accurately machined cylinder and a close fitting piston held in place by a guide pin running in a groove along its length. The cylinder was about 6.5 cm in diameter and its end faces were parallel to within 1μ over this distance. The sample being sectioned was fixed to one end of the piston with metallurgical mounting plastic (North Hill Plastics, London, N.16, Powder No. NHP 2031/19, liquid No. NHP 1844) which was soluble in acetone. Sections were removed by lapping with 1μ diamond paste on plate glass. With a crystal diameter of 0.5 cm, sections could be taken perpendicular to the diffusion direction with an accuracy of better than 0.2%, and as thin as 0.5μ. These limits were obtained using the comparator, and taking a mean of ten readings around the sample surface.

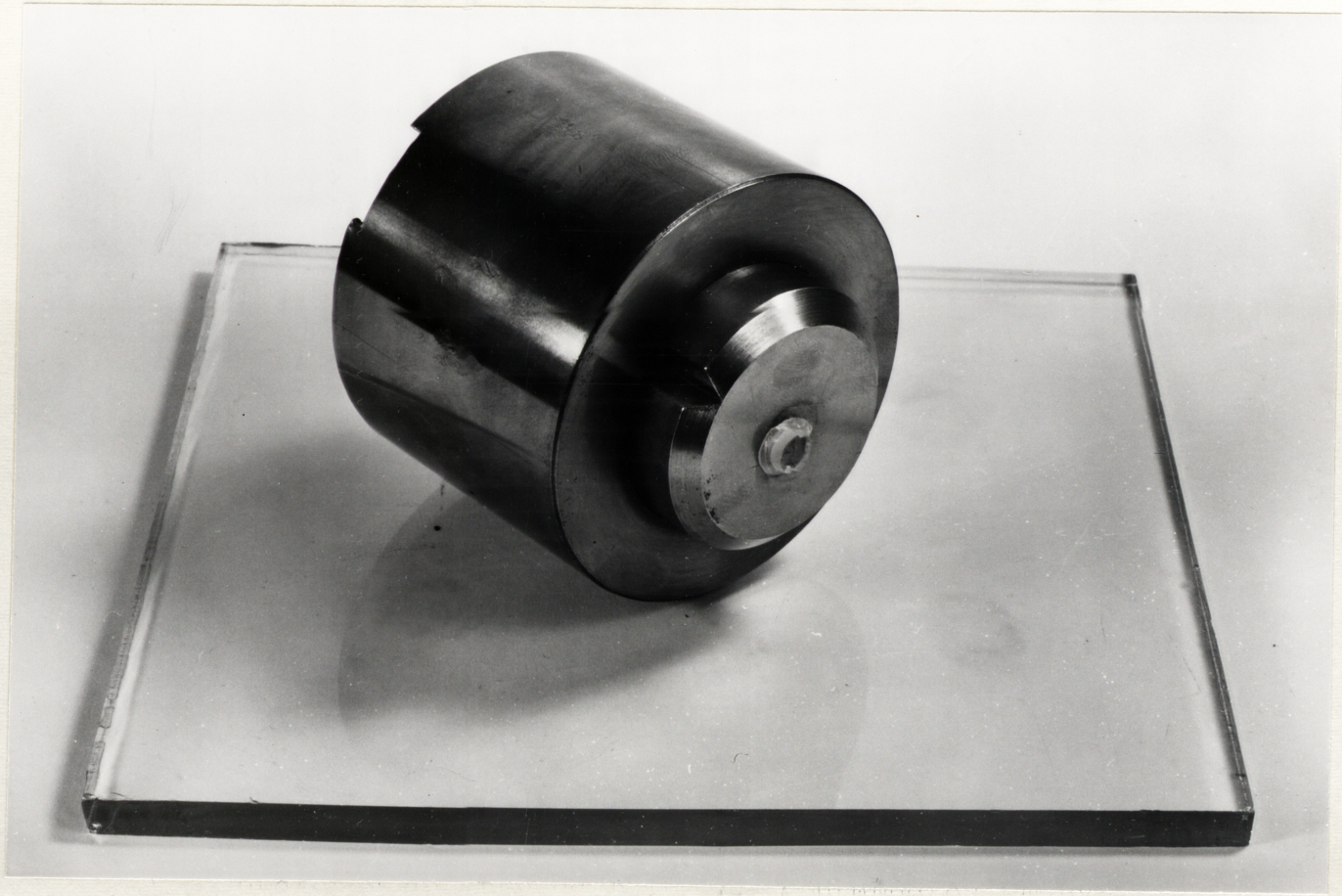

Fig 3.10 Precision grinder used in ^{133}Ba diffusion study

IV. EXPERIMENTAL PROCEDURE

4.1. Preparation of the Diffusion Couples

Magnesium oxide cleaves very readily in the <100> directions. In the first few experiments, crystals were cleaved using a very sharp knife, but in several cases they not only split perpendicularly to the cylinder axis but also parallel to it. In order to produce two near equal pieces, it was found that cutting with a 0.006" diamond wheel was more satisfactory. The crystal was waxed into a jig with its axis perpendicular to the plane of the wheel which was advanced very slowly, about 10 minutes being taken to complete the cut. After cutting, grooves were made in the sides of the cylinders parallel to their axes using a triangular section abrasive stick. This facilitated binding the sandwich together later. The faces exposed by cutting were then polished after any small misalignment with the (cleaved) end faces had been corrected using the precision grinders described. Diamond pastes in grain sizes ranging from 9μ to 1μ were used, producing a good surface for diffusion. (For photomicrographic studies, 0.3μ α-alumina was used on some samples.) For beryllium work, where sections were much coarser, 600 grit carborundum paper backed with plate glass produced a sufficiently smooth surface ($\pm 1\mu$).

The tracer (0.02 ml) in the form of chloride solution

was deposited on each prepared face using a microsyringe. It was found that in using the barium tracer, the addition of a drop of NH_4OH solution facilitated the production of barium oxide when the couple was heated, and greatly reduced the loss of tracer experienced when the more volatile chloride was used alone. The other chlorides, those of calcium and beryllium, convert to the oxides much more readily than barium chloride and there was no need to use chemical means in these cases. Gentle warming was needed to dry the deposits, particularly in the case of the deliquescent beryllium compound. When dry, the two halves of the original crystal were butted tightly together with the aid of another simple jig and held in place with a loop of Pt-13% Rh wire. This helped reduce tracer loss and kept it in intimate contact with the magnesium oxide surface during annealing.

4.2. Annealing the Couples

A couple prepared as described above was slid into a high purity alumina tube and the temperature measuring thermocouple tip placed in contact with it. A brass seal was made to fit over the open end of the tube to hold the thermocouple in place and to prevent the possible escape of radioactive material. This seal was not completely air-tight, so that the pressure remained at one atmosphere throughout the annealing. There was some loss of tracer during the diffusion run,

but it condensed on cooler parts of the tube, its presence being detected by a radiation monitor. There was always sufficient tracer remaining on the crystal surfaces to fulfill the required boundary conditions. In order to avoid possible contamination effects, a new tube was used for each run.

Couples were annealed between 1000°C and 1700°C for periods ranging from one hour to several weeks. Temperatures were controllable to ±5°C at 1400°C with the Cambridge controller and to slightly better limits with the other instruments. In one or two cases, there was a tendency to drift over the duration of the experiment where this was lengthy, but with regular checking using the potentiometer, this could be corrected before it reached serious proportions. The error in the annealing time was negligible as couples could be inserted into furnaces which were already at operating temperature, and only two minutes was required for them to reach 95% of the final temperature. Cooling on withdrawal from the furnaces was very rapid also.

4.3. Determination of Diffusion Profiles

4.3.1. Autoradiography

On withdrawal from the furnace, the ^{45}Ca couple was mounted in metallurgical mounting plastic with its axis parallel to the face of the mount. Grinding then removed material until a section in the diffusion direction perpendicular to

the original diffusion interface was obtained. Careful polishing produced a smooth surface which was then placed in contact with Kodak "Microtex" X-ray film in the dark room. The simple procedure was to use a small piece of perspex as a backing for the film and an elastic band to hold the mount firmly in position on the film. This arrangement was left for several days in a safe place to obtain an exposure of the required density, this having been determined in a series of tests to establish the range over which photographic density varied linearly with exposure time. After development, the image was translated into a concentration vs. penetration graph via a microdensitometer scan. The recorder chart speed was nominally 1" per minute and the film was scanned at 0.25 mm per minute. These two speeds were checked and it was found that the ratio of the distance on the film to the distance on the chart was 0.009962 within an accuracy of 0.16%. Having applied a correction for film shrinkage, the diffusion profile could be analysed as described in paragraph 2.2.2.

4.3.2. Sectioning

The methods used for the determination of profiles for beryllium and barium were similar, differing only in the degree of precision required.

A sandwich, on being removed from the furnace, was cooled and separated into its two parts. The curved surface

and the end face opposite to the diffusion interface were then ground away using 400 grit and 600 grit carborundum paper to a depth greater than the expected value of $3\sqrt{Dt}$. This procedure was intended to ensure that there was no surface contamination adding to the count rate obtained from material which had diffused into the crystal in the axial direction from the original deposit. After cleaning the surfaces, including the grooves used in binding the sandwich together, the crystal was mounted on the grinder to be used, either by gripping it in a nylon collet for the beryllium analysis, or by the use of mounting plastic for barium work. In the latter case, the grinder was placed such that the crystal was pressed to a plate glass surface by the weight of the piston. This ensured that it set in the plastic with its active face parallel to the lapping surface. The beryllium samples, held in the nylon by a threaded brass ring which tightened on to it, could be demounted from the grinder for counting after the removal of each layer. This introduced an error on remounting of about $\pm 1\mu$, which was small compared to the penetrations involved. The much smaller penetrations handled in the barium diffusion work required greater precision and the crystals were never removed from the grinder for counting. Another source of error was the expansion of the grinder cylinder from the heat of the hand while polishing was being done. This was corrected by immersing the cylinder in a water bath at

room temperature after each section had been removed and prior to measuring the amount removed.

The crystal was first counted to determine its total activity. A thin layer was then removed, the grinder cylinder holding the crystal immersed in a water bath, the amount removed measured using a comparator and then the crystal activity determined again. The limits of measurement have already been mentioned in describing the precision grinders (paragraph 3.4). When using the comparator, a mean of at least ten measurements over the surface of the crystal was taken. The counting procedure was as follows:-

(a) the background was counted to, say, 300 counts (at a rate of 15/min),

(b) a standard source (made up with a drop of the appropriate tracer solution which was dried and sealed) was counted to at least 30,000,

(c) the diffusion sample was counted for as long as possible. Near the end of the profile, count rates became rather low and a total of only 3,000 counts could be taken,

(d) the standard source was again counted, and

(e) the background was re-measured.

From these measurements, the activity remaining A(x) at a penetration x, could be calculated in terms of the ratio of the sample count to the standard count. This reduced the

effect of drift in the circuits of the counting equipment to a minimum. D could then be calculated from the A(x) vs. x curve.

V. RESULTS

5.1. Calcium Diffusion

Only one measurement was made with calcium as the impurity in order to check that the crystals were not radically different from those used in previous work. Annealing time for this sample was 853 hours and the temperature was 1308°C. The microdensitometer scan of the autoradiograph obtained from this sample is shown in fig 5.1. This scan was converted to a concentration vs. penetration curve, one half of which is shown in fig 5.2. The slope of the corresponding $(\text{erfc})^{-1}$ C/C_s vs x line, fig 5.3, gave an apparent value for the diffusion coefficient and subtracting a resolution correction resulted in values of 2.6×10^{-12} cm^2/sec and 3.4×10^{-12} cm^2/sec for the coefficients from the two sides of the scan. The resolution correction amounted to 25% of the measured D. These figures fall between the value of 4.5×10^{-12} cm^2/sec derived from the results of Rungis and Mortlock (1966) and the result for 1300°C of 1.44×10^{-12} cm^2/sec obtained recently by Wuensch and Vasilos (1966a).

5.2. Beryllium Diffusion

An example of an integrated diffusion profile where the activity remaining, A(x), is plotted against the penetration distance, x, is shown in fig 5.4. It was noticed in several experiments that A(x) did not fall to zero as would be

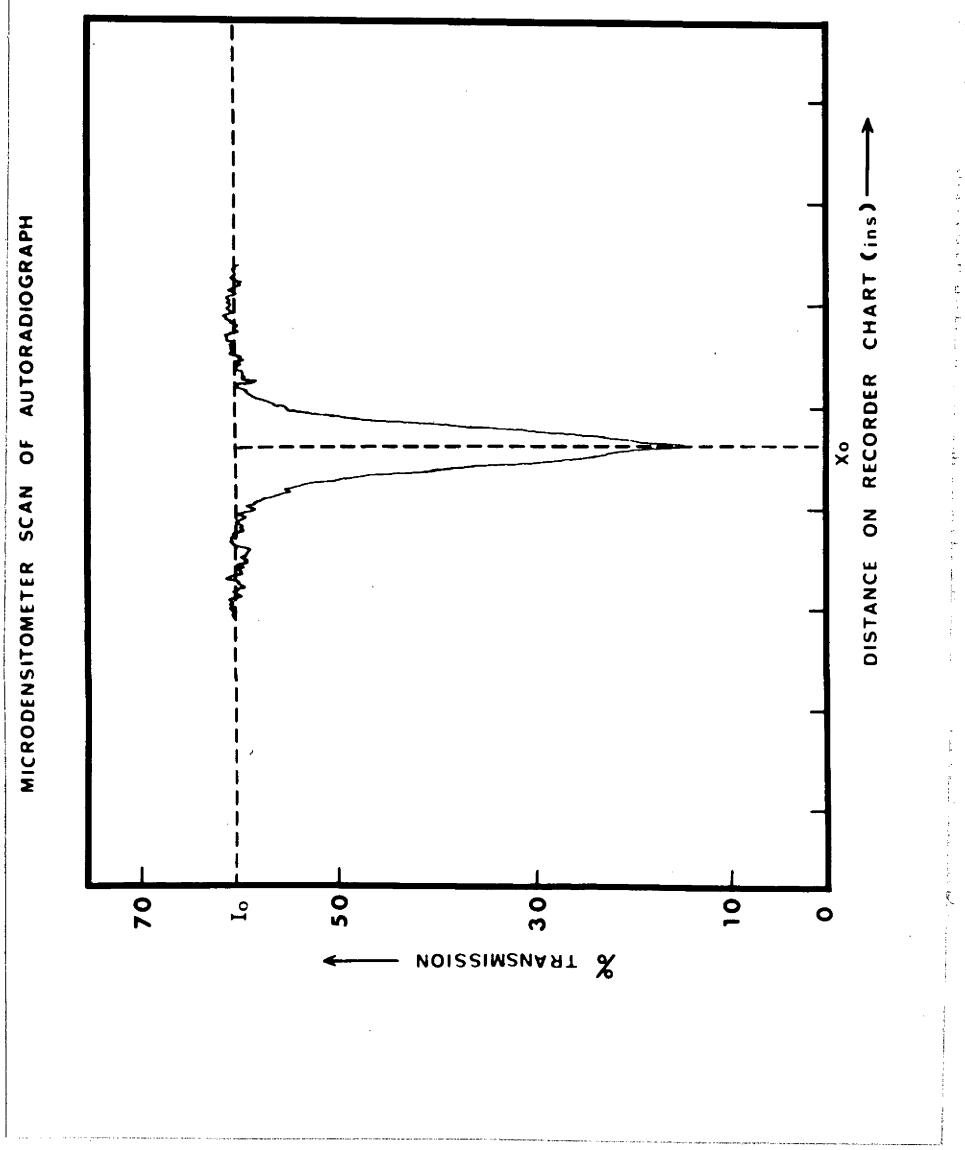

Fig 5.1 Microdensitometer trace of ^{45}Ca diffusion profile.

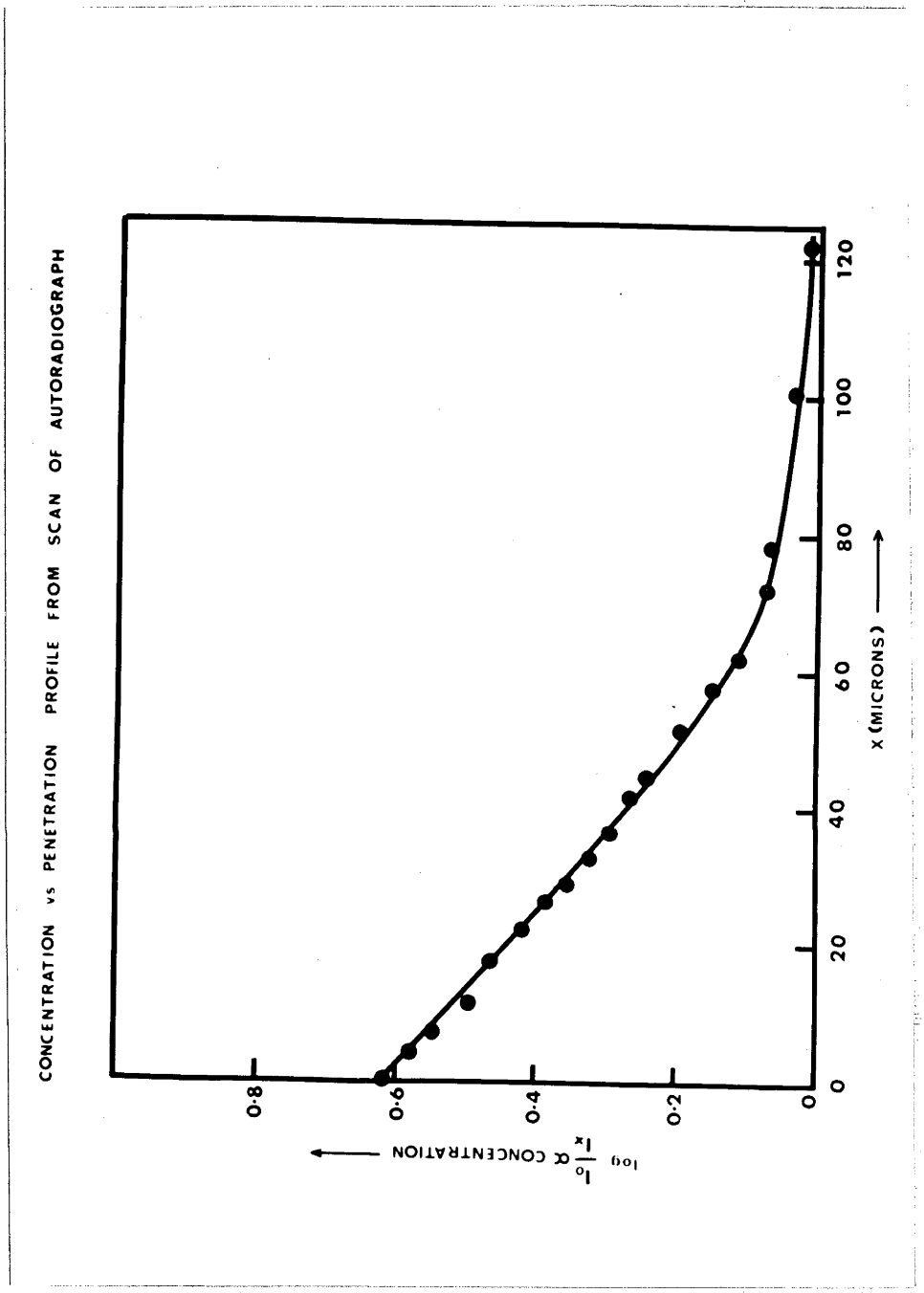

Fig 5.2 Diffusion profile for ^{45}Ca in MgO.

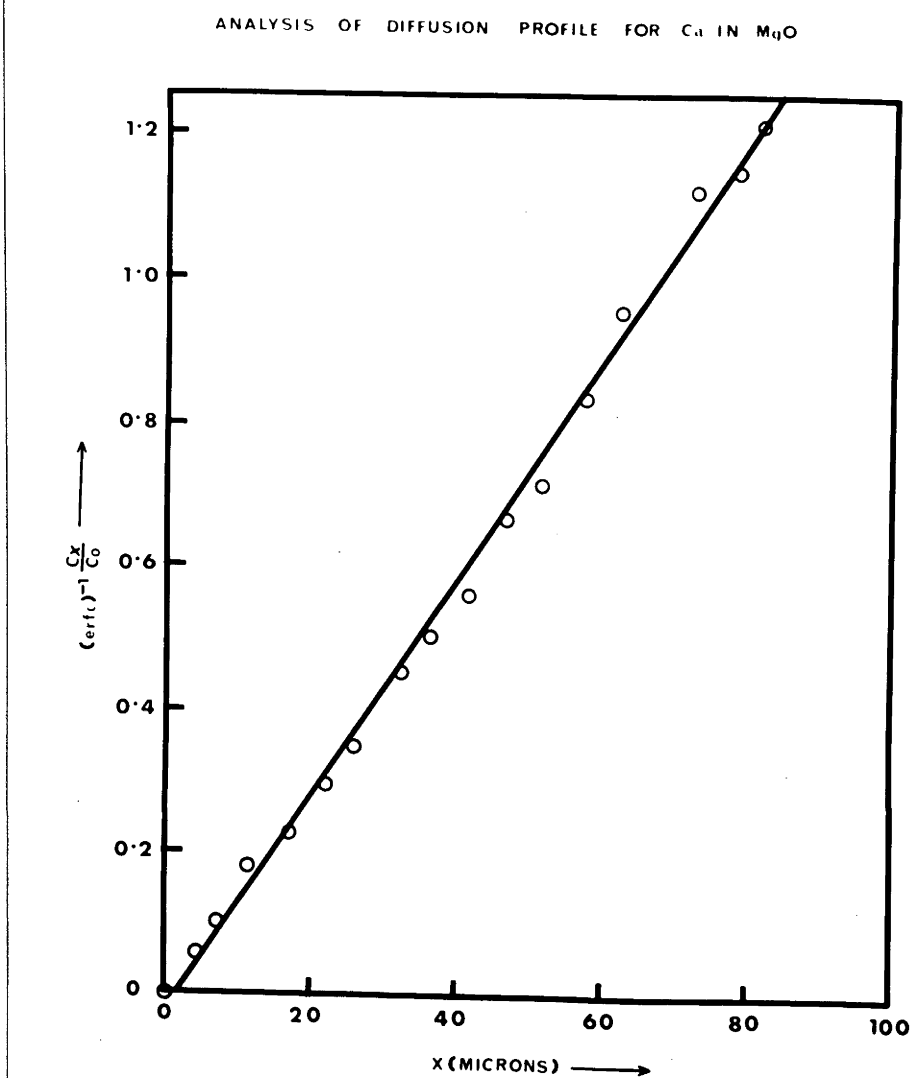

Fig 5.3 Analysis of ^{45}Ca diffusion profile.

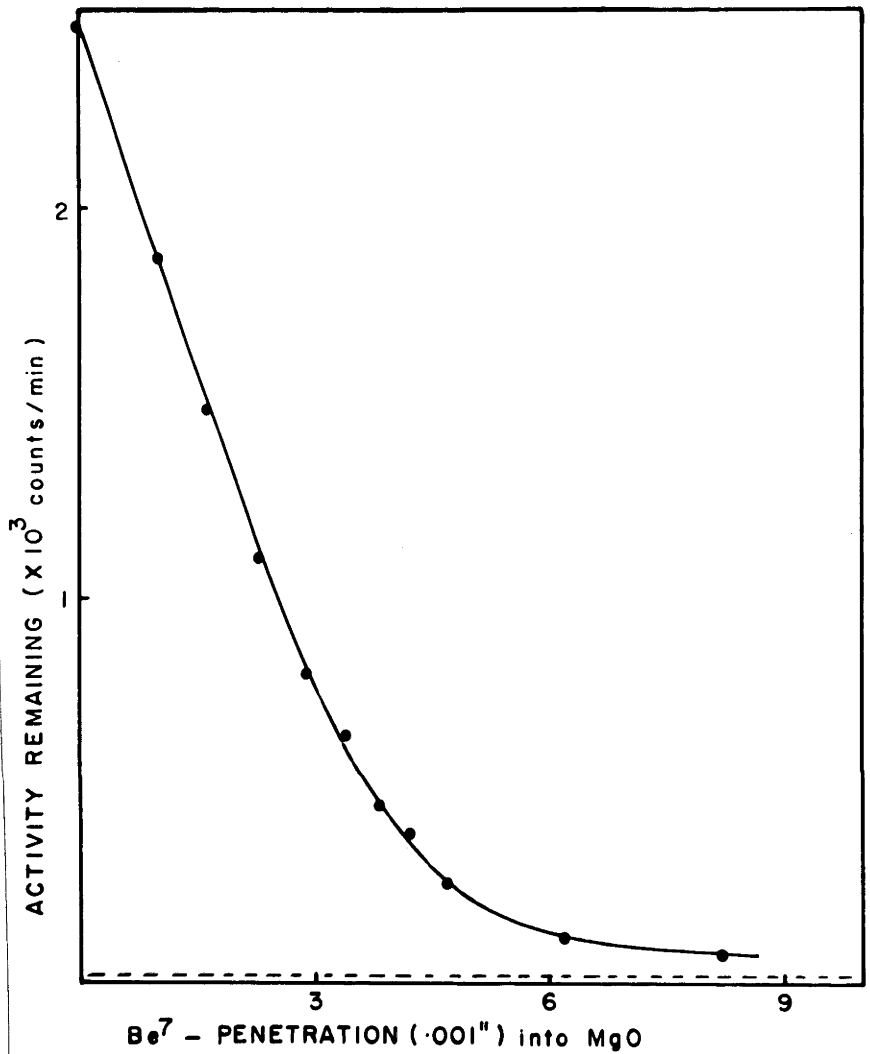

Fig 5.4 An integrated diffusion profile for ^{7}Be in MgO.

expected from theory. The background level is considered to be due to a very small amount of surface contamination, the effect of which is greatly magnified because of the integrating technique used. For example, samples were usually about 2500μ thick in the diffusion direction and hence only one count per minute (about 10^{-12} curies of contamination, compared with an original deposit of about 10^{-6} curies) per 25μ depth could give rise to a background of 100 counts per minute, a figure several times greater than the electronic background. Allowing for this background, the fractional activity remaining, F(x), can be determined, and a graph of $(\text{erfc})^{-1}$ F(x) vs. x plotted. This is a straight line as can be seen in fig 5.5, but in several cases it does not pass through the origin. This is due to a small zero error in x arising from the "crowning" of the section, to which reference was made in paragraph 3.4. The distance B'P (in fig 3.9) is small compared with the total penetrations involved, but it causes the measured thickness of the first section to be too large. This error remains constant in each penetration distance measured and hence, although the slope of the $(\text{erfc})^{-1}$ F(x) vs. x line is unaffected, the line no longer passes through the origin. The slope of this line is $\frac{1}{2\sqrt{Dt}}$ and D can be evaluated. Coefficients obtained in this way are listed in Table 5.1, and a plot of log D vs. 1/T where T is the absolute temperature gives a straight line, fig 5.6. This line

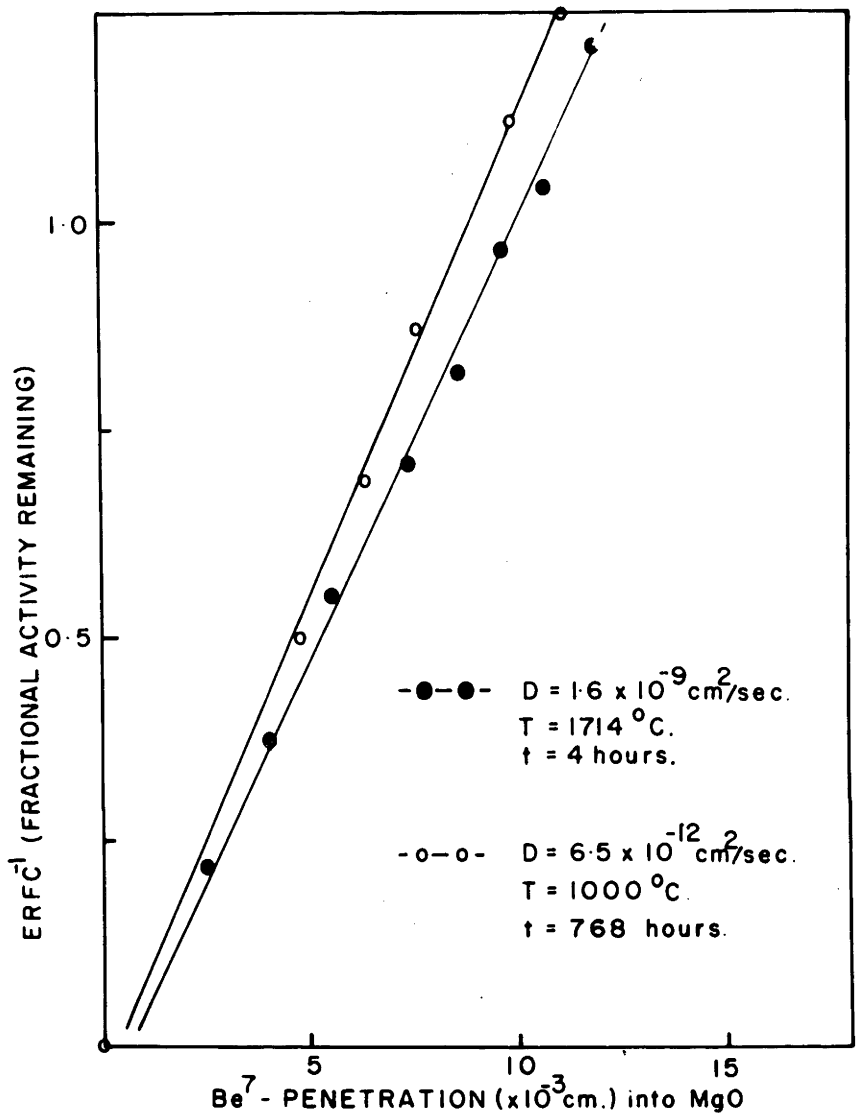

Fig 5.5 Analysis of integrated ^{7}Be diffusion profiles.

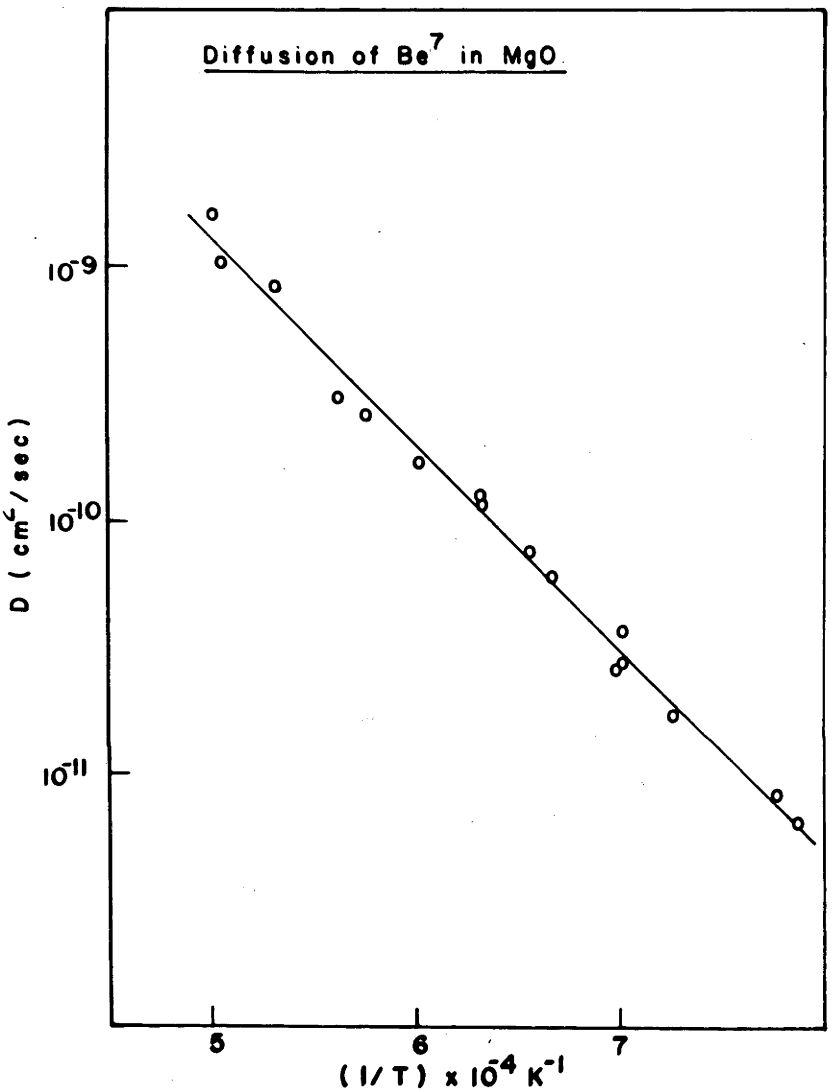

Fig 5.6 Arrhenius plot for ^{7}Be diffusion in MgO

TABLE 5.1

Diffusion of Beryllium in MgO

Temperature (^{o}C)	Annealing time (hr)	Diffusion Coefficient (cm^2/sec)
999	768	6.47×10^{-12}
1016	145	8.39×10^{-12}
1105	336	1.73×10^{-11}
1151	70	3.72×10^{-11}
1151	$222\frac{1}{2}$	2.80×10^{-11}
1158	70	2.60×10^{-11}
1223	$165\frac{1}{3}$	6.08×10^{-11}
1252	46	7.55×10^{-11}
1304	$63\frac{2}{3}$	1.15×10^{-10}
1306	202	1.27×10^{-10}
1388	122	1.69×10^{-10}
1460	498	2.60×10^{-10}
1501	100	3.04×10^{-10}
1604	45	8.43×10^{-10}
1693	23	1.01×10^{-9}
1714	4	1.60×10^{-9}

has been treated by means of the "least squares" method of calculation and can be described by the following equation

$$D = (1.41^{+0.50}_{-0.36}) \times 10^{-5} \exp\left[-(1.60 \pm 0.04)/kT\right] \text{cm}^2/\text{sec} \quad ..(5\text{-}1)$$

where k is Boltzmann's constant in eV/^{o}K and the limits are standard errors from least squares theory.

5.3. Barium Diffusion

An example of an integrated average profile is shown in fig 5.7 for a sample annealed at 1124^{o}C. The meaning of the word "average" will become apparent later. Again the activity remaining, A(x), did not fall to zero at large values of x and the same explanation can be put forward here as was suggested in the last paragraph in relation to the beryllium experiments. Furthermore, this curve should be a smooth line described by an integrated error-function complement in accordance with the calculations in paragraph 2.2.4. However, if a plot of $(\text{ierfc})^{-1}$ F(x) vs x is made from the experimental points, having first subtracted the background line, the graph shown in fig 5.8 results. From this it is evident that the experimental curve can be divided into two regions, in addition to the region of surface phases, the limit of which is defined by the very sharp fall in count rate over the values of x from 0μ to 8.0μ. The two regions of diffusion are marked by an abrupt change of slope (at 20μ

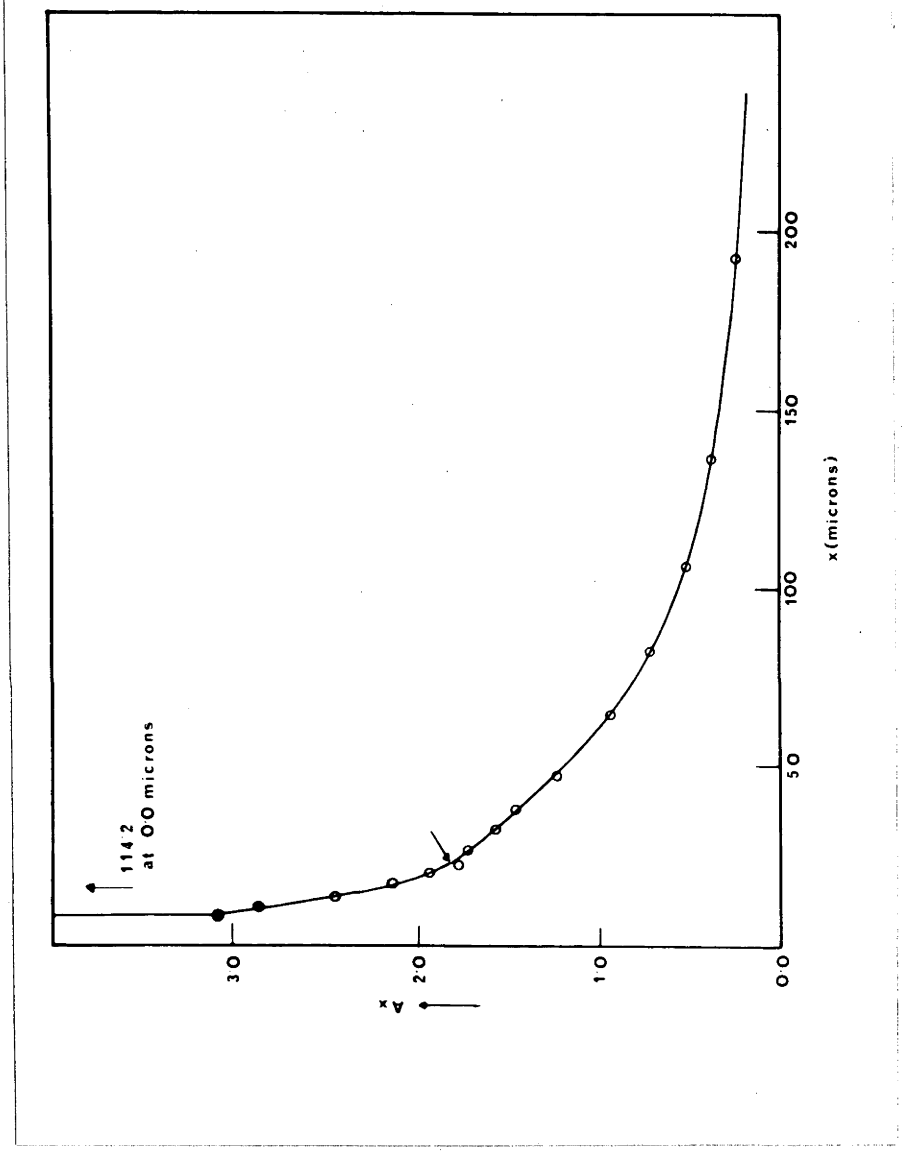

Fig 5.7 An integrated "average" diffusion profile for ^{133}Ba in MgO (T = 1124°C)

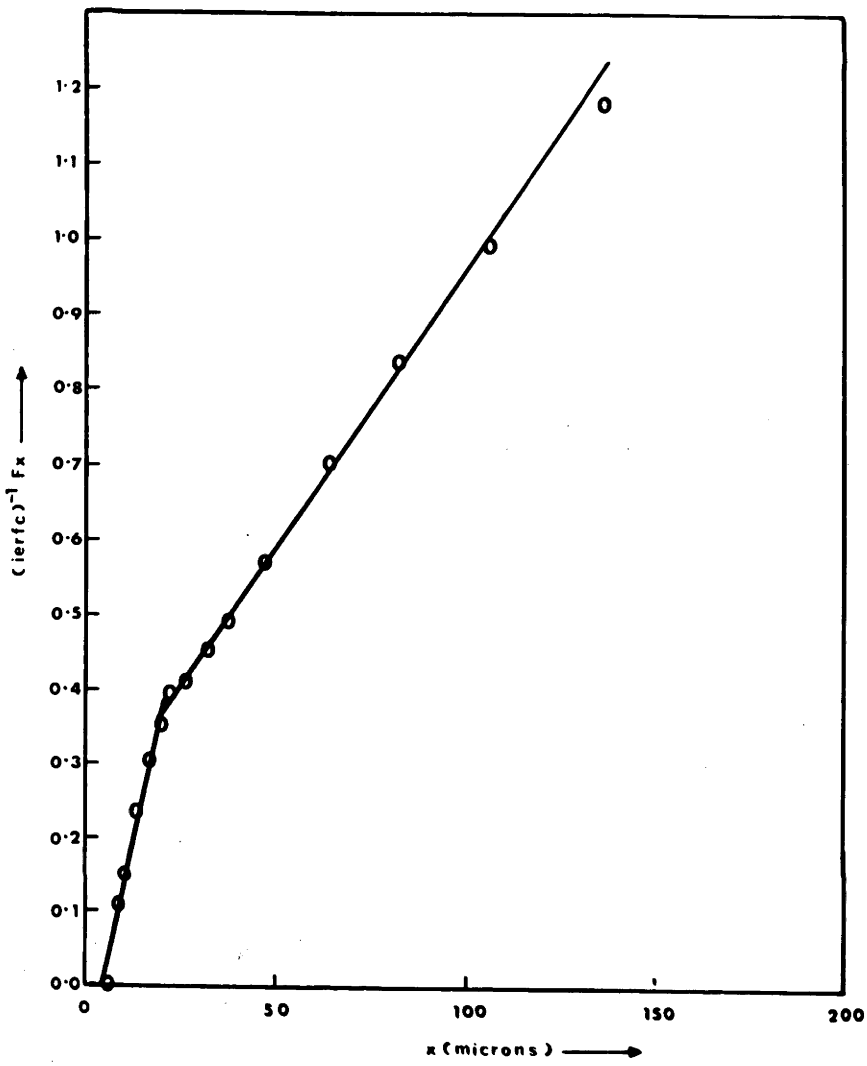

Fig 5.8 Analysis of an "average" ^{133}Ba diffusion profile.

in this sample) in the $(\text{ierfc})^{-1}$ F(x) vs. x plot. The corresponding point in the experimental curve is indicated by an arrow in fig 5.7.

It is apparent then, that there are two processes involved in the diffusion of Ba in MgO and that the diffusion coefficient derived from the full experimental curve is an "average" coefficient. For reasons discussed later, it is believed that such coefficients are dislocation-influenced and the symbol $D_{\ell + d}$ will be used in referring to them. A plot of log $(D_{\ell + d})$ vs 1/T is shown as line "b" in fig 5.12. The "least squares" equation describing it is

$$D_{\ell + d} = (6.3^{+4.2}_{-2.5}) \times 10^{-5} \exp\left[-(1.85 \pm 0.07)/kT\right] \text{ cm}^2/\text{sec} \quad (5\text{-}2)$$

The limits are again standard errors derived from least squares theory.

The steeper region of the experimental curve (extending to a penetration of about 20μ for the 1124°C sample) is believed to be due to true lattice diffusion. Re-plotting this region on a larger scale (e.g. figs 5.9 and 5.10) it is possible to calculate lattice diffusion coefficients assuming that a "background", represented by the extrapolation of the dislocation "tail" back to x = 0, can be subtracted from the experimental curve. The $(\text{ierfc})^{-1}$ F(x) vs. x graphs for two runs treated in this way are shown in fig 5.11. These lines

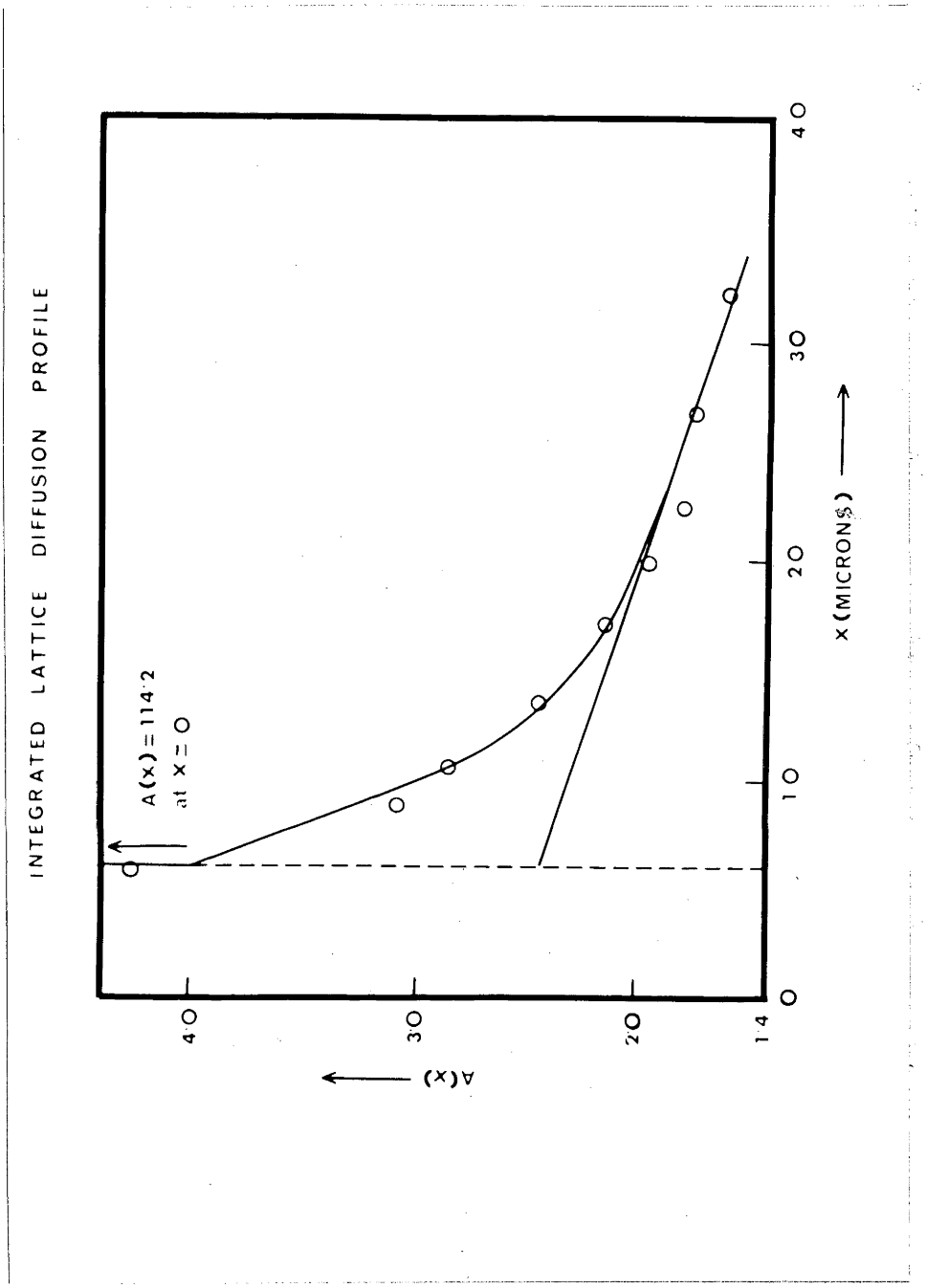

Fig 5.9 An integrated lattice diffusion profile for ^{133}Ba in MgO ($T = 1124^{o}C$)

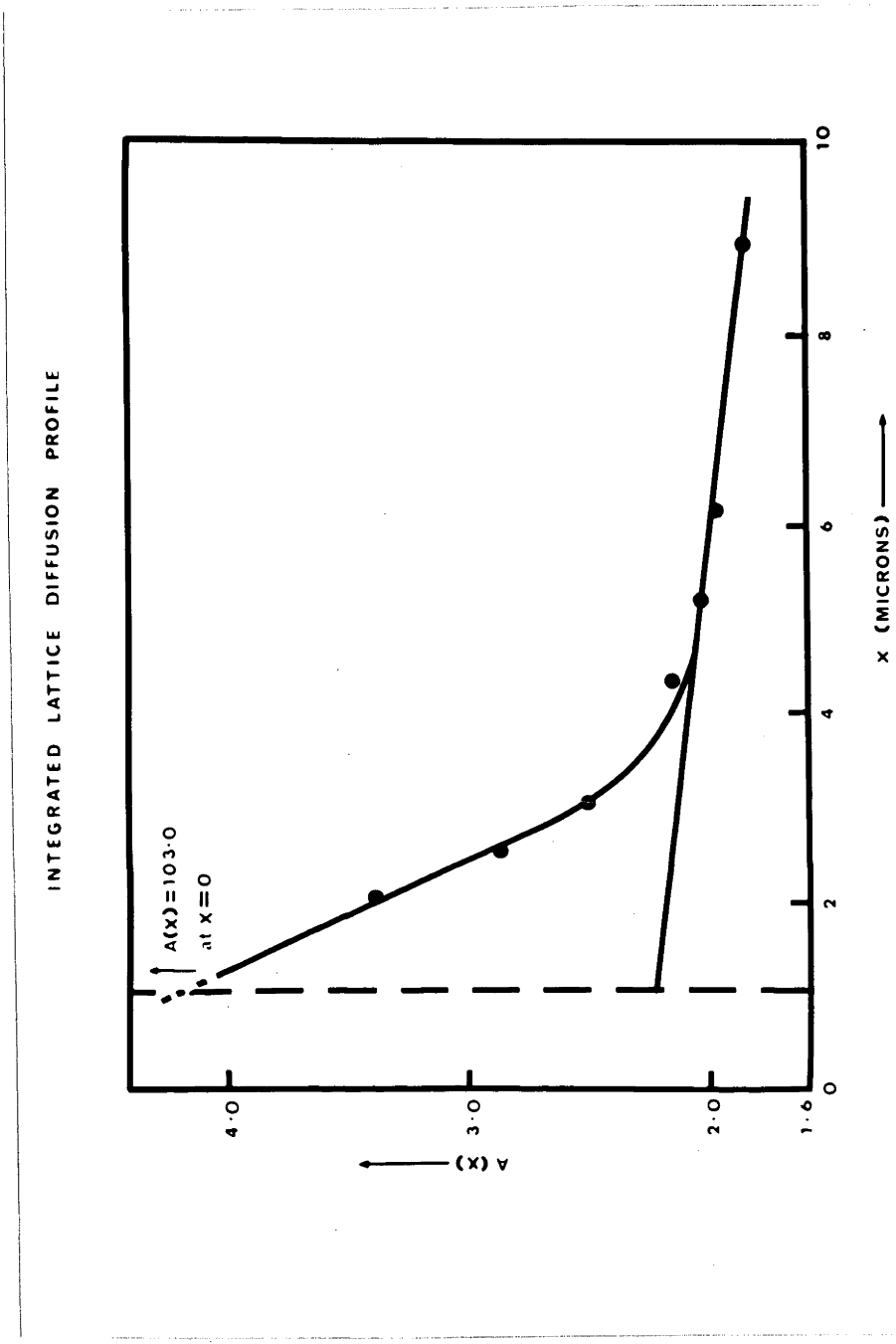

Fig 5.10 An integrated lattice diffusion profile for ^{133}Ba in MgO ($T = 1008^{o}C$)

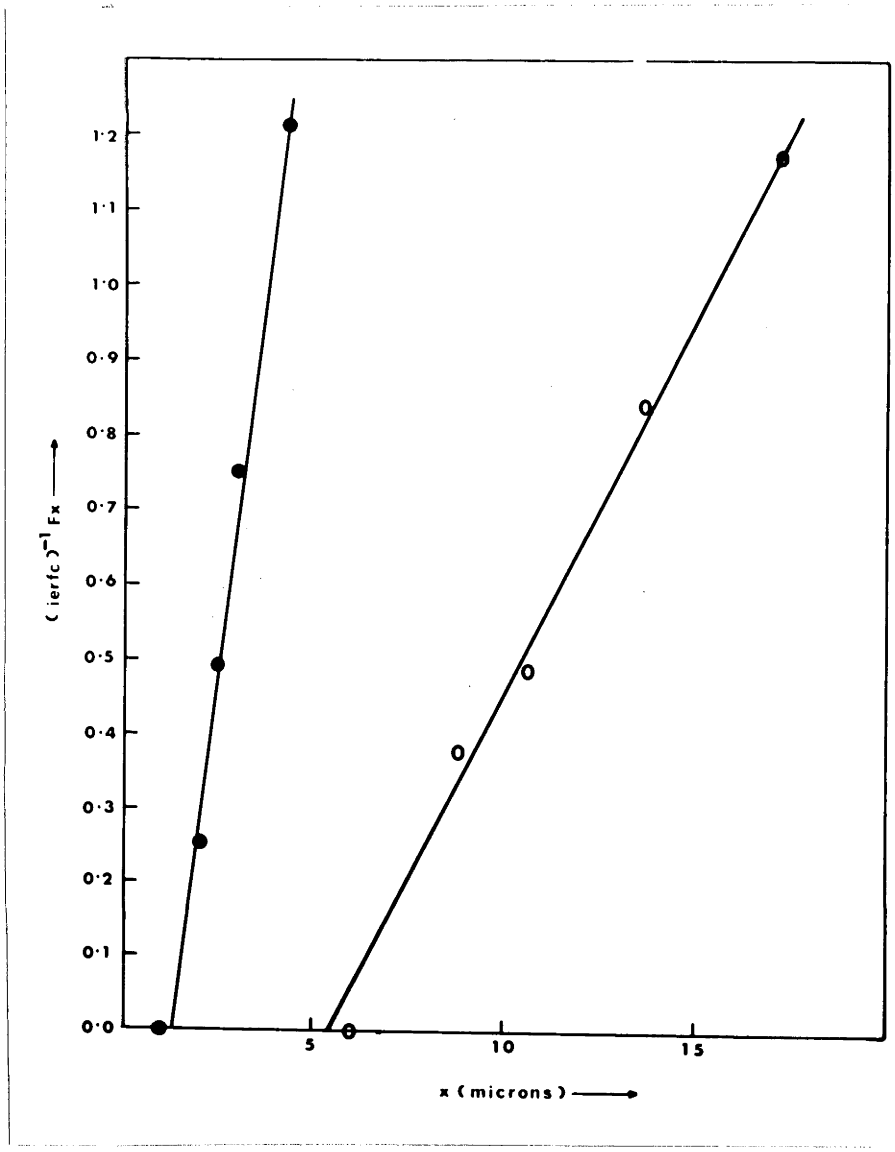

Fig 5.11 Analysis of lattice diffusion profiles for ^{133}Ba in MgO

again do not pass through the origin. The more refined grinding method used in the barium experiments eliminated the "crowning" effect observed previously during the study of beryllium diffusion, but due to the low solubility of BaO in MgO, a surface zone of undissolved tracer of finite thickness was always present. Under these conditions, the solution to the diffusion equation is given by equation (2-4). Therefore $(\text{ierfc})^{-1}\ F(x)$ is zero at x_s, but the slope of this function plotted against x is unaffected. A graph of the logarithm of these coefficients (D_ℓ) against 1/T (line "a" in fig 5.12) is described by the equation

$$D_\ell = (0.07\ ^{+0.03}_{-0.02}) \exp\left[-(3.38 \pm 0.05)/kT\right] \quad \ldots\ldots \quad (5\text{-}3)$$

A summary of the experiments conducted and the diffusion coefficients obtained is shown in Table 5.2.

It should be pointed out that dislocation diffusion coefficients would not be accurately described by the treatment given. The concentration profile for grain boundary diffusion has been treated simply by Fisher (1951) and can be applied here. The solution is two dimensional, but the average concentration $\overline{C}$ at a penetration distance x can be evaluated, taking the average over the lateral dimension i.e. over the dimension parallel to the deposited surface layer of diffusant. This is of the form

$$\overline{C} = (\text{constant}) \times e^{-Kx} \quad \ldots\ldots\ldots \quad (5\text{-}4)$$

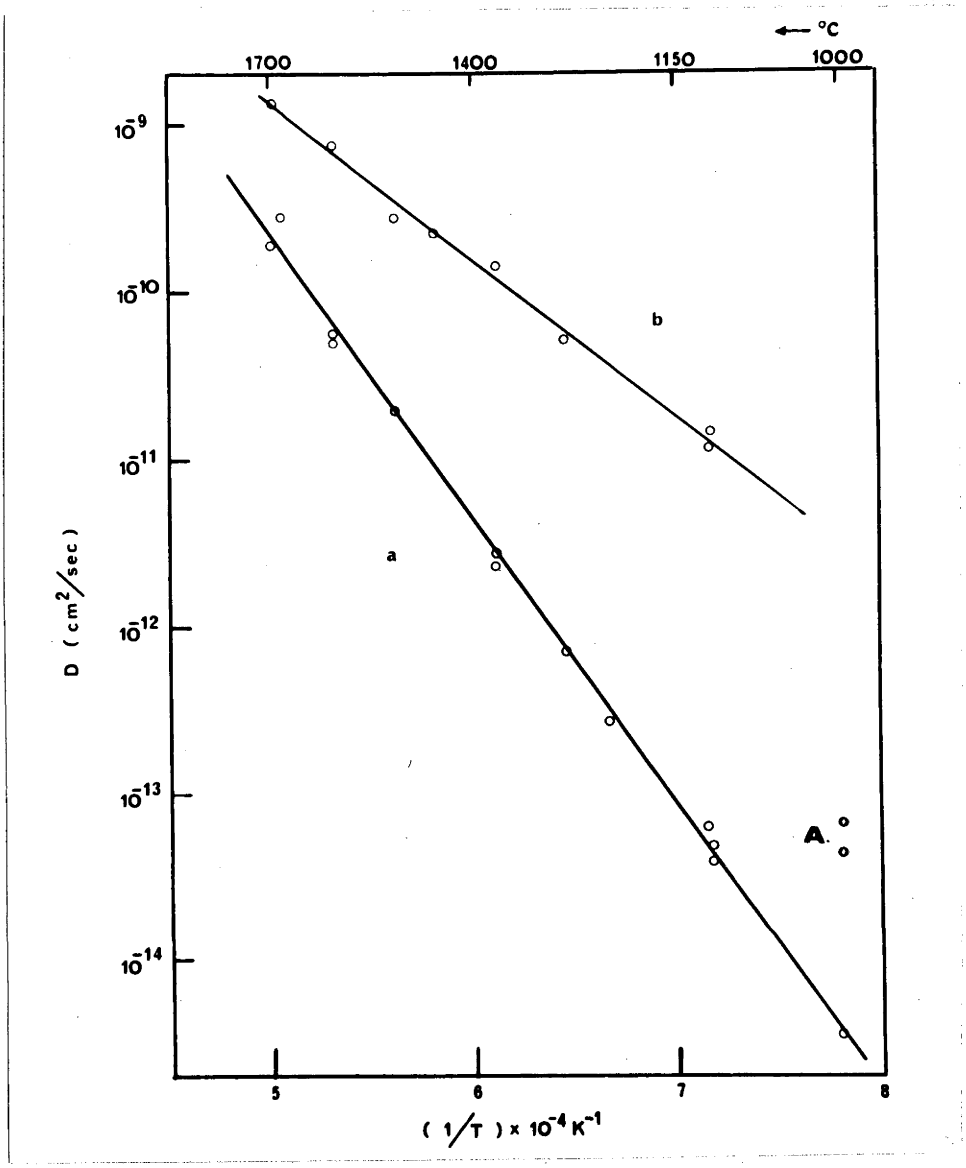

Fig 5.12 Arrhenius plots for (a) lattice diffusion and (b) dislocation-influenced diffusion, of ^{133}Ba in MgO.

TABLE 5.2

Diffusion of Barium in MgO

Temp °C	Time (hr)	D_ℓ (cm^2/sec)	$D_{\ell + d}$ (cm^2/sec)
1008	1319	3.56×10^{-15}	4.50×10^{-14}
"	"	3.62	6.95×10^{-14}
1120	840	5.12×10^{-14}	1.47×10^{-11}
"	"	4.02	
1124	1075	6.51	1.16×10^{-11}
1228	604	2.70×10^{-13}	
"	"	2.64	
1277	$62\frac{1}{2}$	7.20	5.17×10^{-11}
1361	24	2.69×10^{-12}	1.46×10^{-10}
"	"	2.70	
"	96	2.35	
1446	$18\frac{1}{2}$		2.22×10^{-10}
1507	5	1.93×10^{-11}	2.74×10^{-10}
"	"	2.13	
1608	20	5.02	
"	"	5.79	7.73×10^{-10}
1703	13	2.82×10^{-10}	
1724	$1\frac{1}{3}$	1.89	1.38×10^{-9}

where $K = \frac{1}{(\pi Dt)^{1/4}} \left(\frac{2D}{\delta D_g}\right)^{\frac{1}{2}}$, D being the lattice coefficient and D_g the grain boundary coefficient. δ is the width of the grain boundary. The average diffusion coefficient, $D_{\ell + d}$, is a combination of pipe diffusion and lattice diffusion. For the sake of comparison with previously obtained results, the overall diffusion profile has been treated using lattice diffusion theory. An estimate of the diffusion coefficient for pipe diffusion is given later. Further, the detection or otherwise of the discontinuity in the $(\text{ierfc})^{-1}$ F(x) vs x plot will depend in general on the ratio of D_ℓ to $D_{\ell + d}$ and also on the annealing time t.

5.4. Errors in Individual Diffusion Coefficients

5.4.1. Temperature

We require the percentage variation of the diffusion coefficient D with a change in temperature of $\pm 5^{\circ}C$, since this is the estimated control obtained during annealing. The Arrhenius equation is

$$D = D_o \exp\left(-\frac{Q}{kT}\right) \qquad \ldots\ldots \quad (5\text{-}5)$$

$$\text{Hence} \quad \Delta D = \frac{D_o Q}{kT^2} \cdot \exp\left(-\frac{Q}{kT}\right) \cdot \Delta T \qquad \ldots\ldots \quad (5\text{-}6)$$

$$\text{or} \quad \frac{\Delta D}{D} = \frac{Q}{kT^2} \cdot \Delta T \qquad \ldots\ldots \quad (5\text{-}7)$$

For $T = 1000^{\circ}C$ and $Q = 1.6$ eV we have from this, $\frac{\Delta D}{D} = 0.057$.
For $T = 1600^{\circ}C$ and $Q = 1.6$ eV, the fractional error is 0.027.

Thus the percentage error in D varies from about ±3% to ±6%. In the case of barium diffusion the errors would be twice this, for an activation energy of 3.38 eV.

5.4.2. Duration of Annealing

The couples were inserted into furnaces already at temperature and reached 95% of the final temperature in two minutes, even for a run at 1724°C. Cooling was very rapid and its effects can be neglected. In one instance, the annealing period was as short as 80 minutes and so the largest time error was of the order of 2-3%. All other annealings were of 4 hours and over, producing errors generally of less than 0.2%.

5.4.3. Penetration Distances

In the determination of barium profiles, the grinder was subject to small temperature variations over the course of the experiment, but the comparator stand was made of the same material, so these room temperature fluctuations, usually only 3°C or less, had little effect on the relative distances measured. A mean of ten readings made with the comparator after polishing gave each measurement to ±0.2μ. Distances were obtained by subtracting each measurement from an original taken before polishing began. In an average penetration of 20μ, x could therefore be determined to ±2%. This gave an error in D of ±4% for lattice diffusion. For dislocation influenced diffusion the distances involved were greater than 60μ reducing the error in D to about 1%.

5.4.4. Errors Arising from Counting and Calculations

Individual measurements of the tracer activity were accurate to 3% or better depending on the count rate. In some cases this was very low and only 3000 counts could be taken, because beyond a certain time limit the stability of the counting equipment became a significant factor. Other work in the laboratory could affect the background and temperature of the room. The activity A(x) used in calculations was the ratio of the sample count rate to a standard count, and by this means the effect of random fluctuations in counting conditions was minimised.

The estimation of A(o) and the background lines of the integrated profiles was the main source of error in determining F(x). It is considered that in an average profile, A(o) could be found to $\pm 7\%$ and values of A(x) to similar limits. The limits on F(x) were therefore $\pm 10\%$.

The functions $(\text{erfc})^{-1}$ u and $(\text{ierfc})^{-1}$ u are plotted against u in figs 5.13 and 5.14 respectively. For the beryllium diffusion experiments, u = F(x) and to see the effect of errors in F(x) on $(\text{erfc})^{-1}$ F(x) we can write

$$\Delta\,(\text{erfc})^{-1}\,F(x) = \frac{d(\text{erfc})^{-1}\,F(x)}{d\,F(x)} \cdot \Delta F(x) \qquad \ldots\ldots \quad (5\text{-}8)$$

For values of u greater than 0.2, $(\text{erfc})^{-1}$ u vs. u is nearly linear and the slope is approximately unity. The error in

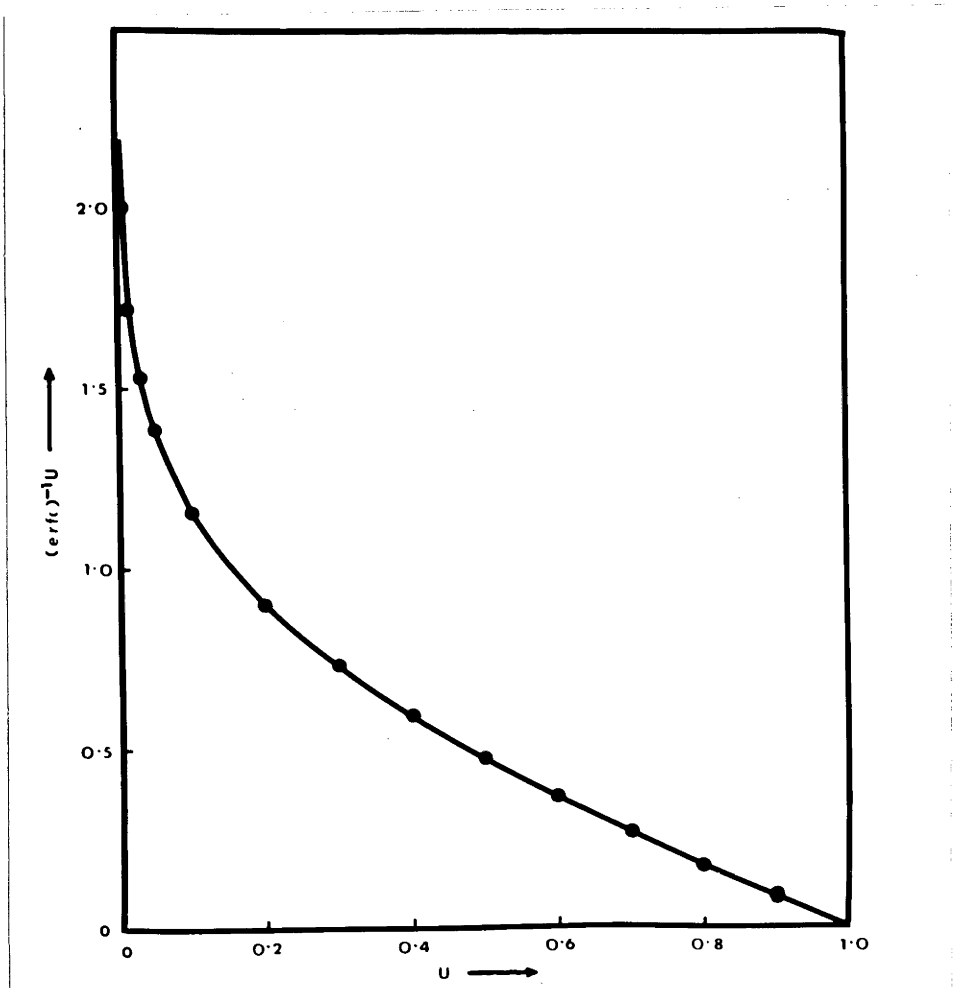

Fig 5.13 Theoretical plot of $(erfc)^{-1}$ u vs. u

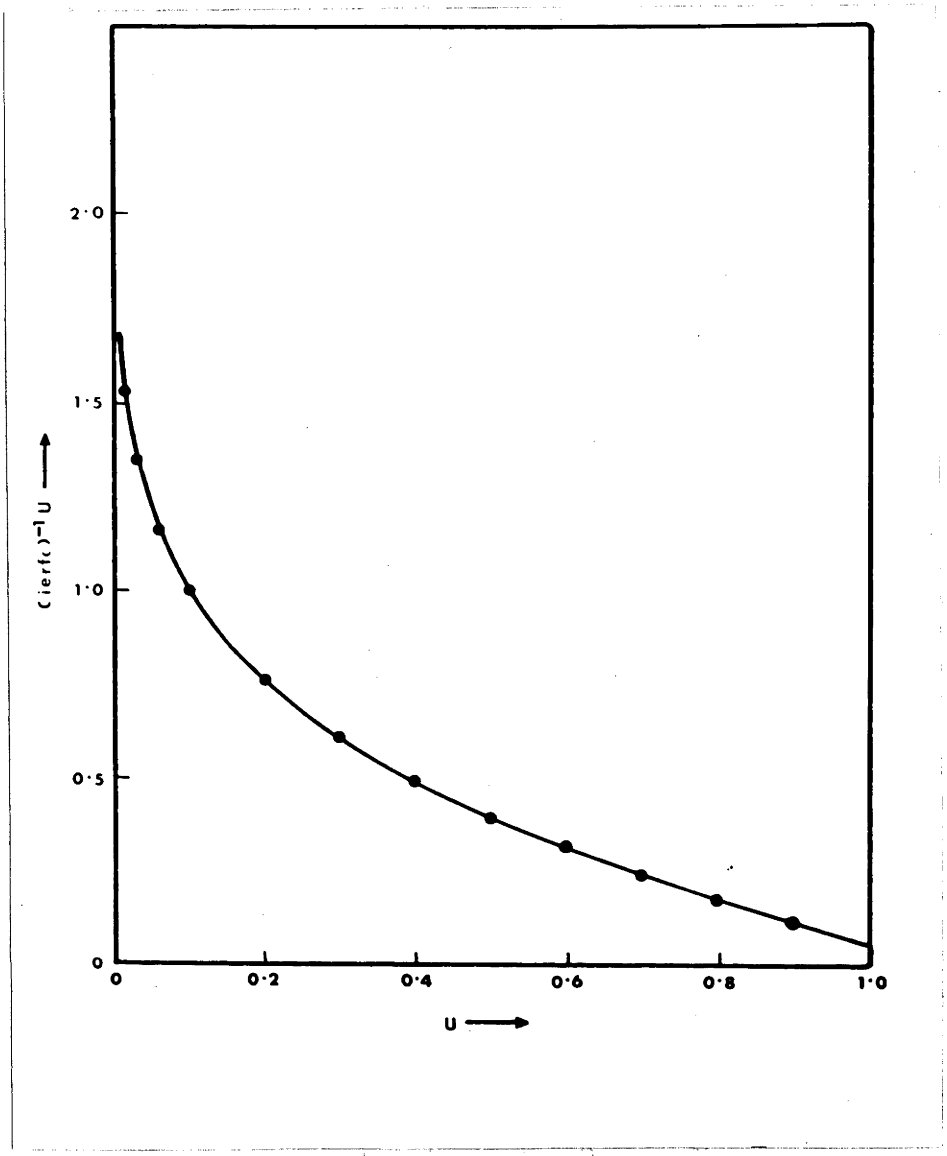

Fig 5.14 Theoretical plot of $(ierfc)^{-1}$ u vs. u

$(erfc)^{-1}$ F(x) is therefore the same as the error in F(x), namely $\pm$10%. For u < 0.2, the slope of $(erfc)^{-1}$ u vs. u increases rapidly and hence the error in $(erfc)^{-1}$ F(x) becomes very large for small F(x). A small value of F(x) corresponds to large values of x. In practice, points on the $(erfc)^{-1}$ F(x) vs. x graph for $(erfc)^{-1}$ F(x) > 1.2 were regarded as unreliable.

A similar argument can be applied in the barium analyses (although an extra constant is involved). For u > 0.2, the slope of $(ierfc)^{-1}$ u vs. u is nearly linear and a little less than unity. Therefore values of $(ierfc)^{-1}$ F(x) less than 1.0 say, can be regarded as again being accurate to $\pm$10%. Again for small values of F(x) experimental points on the $(ierfc)^{-1}$ F(x) vs. x graph become unreliable.

In some cases, it was necessary to estimate the position of the interface between the MgO and surface phases. By careful sectioning, this could be determined to within $\pm 1\mu$ and over this distance, the slope of the $(ierfc)^{-1}$ F(x) vs. x line (for Ba) and the $(erfc)^{-1}$ F(x) vs. x line (for Be) was unaffected.

D is derived from the slope of $(erfc)^{-1}$ F(x) vs. x and $(ierfc)^{-1}$ F(x) vs. x graphs. Although each individual point contains an error which could be as high as 17%, graphing

the results reduces the error to no more than ±8% and several plots were a good deal better than this.

5.4.5. Summary of Principal Errors

The principal errors and the corresponding contributions to the overall error in individual values of D are listed in Table 5.3.

TABLE 5.3

Source of error	Magnitude	Effect on D
1. Temperature	± 5°C	± 6%
2. Time	± 2 mins	negligible
3. Slope of $(\text{erfc})^{-1}$ graph or $(\text{ierfc})^{-1}$ graph	± 8%	± 16%

Item 3 in the table includes counting and penetration errors, and it occurs as a square in the final calculation

$$D = \frac{1}{4 \cdot t \cdot (\text{slope})^2} \qquad \ldots\ldots \quad (5\text{-}9)$$

Referring to item 2, it should be noted that in one experiment the time error was 2.5%. However, calculating the overall error by taking the square root of the sum of the squares of each contribution, shows that this makes a difference of little more than 0.1%. In all other cases, the time contribution was much less. The error in each individual D is

therefore of the order of $\pm$17%. The errors quoted in the Arrhenius equations however, are based on the least square scatter of the points, as mentioned previously.

VI. DISCUSSION

6.1. Diffusion of Be in MgO

The activation energy for Be diffusion in MgO does not agree with the correlation (equation 1-16), a result which is not entirely unexpected in view of the high predicted value of 15.7 eV. The value of D_o, at the same time, is very low and has a similar value (1.41×10^{-5} cm^2/sec) to those obtained in earlier work. Before considering the very interesting results obtained for barium diffusion, it is worth commenting on this result. Beryllium is an extremely small ion and its diffusion may proceed by a different mechanism to other impurity diffusion. There are two possible views that can be taken to explain the beryllium result. The correlation was proposed on the basis of activation energies obtained for divalent ions diffusing, presumably, by the same mechanism. This mechanism is likely to be a substitutional one. The break down of the correlation for Be could be explained by the existence of a different mechanism, namely, an interstitial process. An examination of a crystal model revealed that Be^{2+} would indeed fit into the MgO lattice interstitially. However, the existence of a charged interstitial would require an associated cation vacancy to preserve charge neutrality. (The alternative, an associated anion interstitial can be excluded merely on the basis of ion size.) Diffusion would thus involve the movement of an impurity interstitial/cation

vacancy complex. This would be expected to require a positive entropy of activation yielding a "normal" value for D_o and this is not found. In this case, also, an activation energy of 1.6 eV may be too low.

The alternative is to assume that the correlation applies to all substitutional diffusion and is not dependent on the state of ionisation of the diffusing species. If the values of r and α for the neutral atom Be are used, the correlation in fact predicts the experimental result exactly. But in this case, an interstitial mechanism is unlikely because of the increased value of r for the atom. We would therefore have a neutral atom on an Mg^{2+} site, and again it would be necessary to consider some sort of complex, perhaps as associated anion vacancy. However, the apparent entropy of activation for the diffusion of such a complex again should be positive because of the increased disorder required for its motion. This in turn would give a "normal" value for D_o and this is contrary to observation.

Neither of the above theories are very satisfactory, then. Perhaps it could be pointed out that if charge neutrality were not preserved, then either of the two arguments becomes quite feasible. Also the values of Q and D_o indicate that dislocations could be influencing diffusion. However, further work should be done to clarify the problem set by this system.

6.2. Diffusion of Ba in MgO

To explain the result obtained for barium diffusion, we have two possible alternatives. Either (a) there exists two lattice diffusion mechanisms or (b) we have lattice diffusion with dislocation-influenced diffusion. A similar problem has been discussed previously in relation to diffusion in metals (Le Claire, 1965). It must also be added that some metal systems show, in addition, a third near-surface diffusion region (Lundy et al., 1965) and that, if it exists in MgO, the present technique would not be capable of resolving it in detail. The presence of dislocations in the so-called anomalous metals, γ-U, β-Ti and β-Zr, is regarded as being one feasible explanation of the observed diffusion parameters, namely, low D_o values and activation energies that are about half those for cation self-diffusion (Kidson, 1965). In view of the large size of the Ba atom, it is unlikely that it would diffuse by any means other than substitution and it is therefore reasonable to consider dislocation effects. That the presence of dislocation structures could enhance diffusion is confirmed by the fact that the charge associated with them in MgO has been found to be positive (Rueda and Dekeyser, 1961). This could lead to cation vacancies in the adjacent lattice to preserve electrical neutrality, as mentioned in paragraph 3.1.3.

To estimate a dislocation density which would account for the observed Ba diffusion coefficients, two methods can be used:-

1. It will be noted that the "average" coefficients for each half of the couple annealed at 1008°C (points A in fig 5.12) fall well below the Arrhenius plot describing dislocation-influenced diffusion (line "b"). This can be interpreted on the basis of theories concerning high-diffusivity paths (Hart, 1957; Ruoff and Balluffi, 1963; Harrison, 1961) as meaning that at this temperature the value of $2\sqrt{D_\ell t}$ is less than the mean distance between dislocations, d. By this reasoning it can be said that d must lie between the values of $2\sqrt{D_\ell t}$ at 1008°C and 1124°C, that is, between 2.6μ and 7.0μ respectively. These limits then correspond approximately, to a range of 2×10^6 per cm^2 to 14×10^6 per cm^2 for the dislocation density.

2. In the temperature range studied, the lattice diffusion coefficients are 10-1000 times smaller than the dislocation-influenced coefficients. It is reasonable then to assume that the slope of the Arrhenius plot at low temperatures for the dislocation-influenced process is dominated by the activation energy for pipe diffusion (Kidson, 1965). Assuming that pipe diffusion is described by the Arrhenius equation

$$D_{pipe} = D^{o}_{pipe} \exp - \frac{Q}{kT} \qquad \ldots\ldots \quad (6\text{-}1)$$

and putting D^{o}_{pipe} equal to unity (Le Claire, 1965) it is possible to calculate D_{pipe} for a given absolute temperature T. Two such calculations give, for 1124°C and 1507°C,

$$1124^{\circ}C \qquad D_{pipe} = 3.0 \times 10^{-7} \text{ cm}^2/\text{sec}$$

$$1507^{\circ}C \qquad D_{pipe} = 7.2 \times 10^{-6} \text{ cm}^2/\text{sec} \qquad \ldots\ldots \quad (6\text{-}2)$$

In the general case, the Hart-Mortlock equation gives the total diffusion coefficient (Hart, 1957; Mortlock, 1960) as

$$D_{total} = D_{\ell} + f \frac{C_d}{C_o} D_{pipe} \qquad \ldots\ldots \quad (6\text{-}3)$$

where f is the fraction of atoms (ignoring the existence of two species) on dislocation sites and C_d/C_o is the ratio of the fractional concentration of solute on dislocation sites to that on perfect lattice sites. The second term represents the dislocation-influenced component of the total coefficient and can be identified with $D_{\ell + d}$. As mentioned above, in this case D_{ℓ} is small and $D_{\ell + d}$ is approximately equal to D_{total}. Taking a middle value of 10 for C_d/C_o, f is found to be approximately 10^{-6} for each temperature. Assuming 10 atoms per dislocation cross section, this gives 10^8 per cm^2 for the dislocation density. For a range of pre-exponential factors of 0.1 to 10 cm^2 sec^{-1} and C_d/C_o of 10 to 100, this gives the density a range of 10^6 - 10^9 per cm^2, in agreement with the first calculation.

The energy of formation of an edge dislocation in metals is approximately 10 eV per atom along a dislocation line (Dekker, 1962). The configurational entropy is very small and about 10^{-6} kT. This means that the density of dislocations in thermal equilibrium essentially vanishes, a very different result to that applying to "point" defects. Dislocations then, tend to be "frozen in" by mutual interaction and their density is determined mainly by the past history of the sample concerned. This is in agreement with the calculations above in which f was found to be the same for both 1124°C and 1507°C.

Experimental evidence for the presence of dislocations was found in the photomicrographic studies carried out on several of the crystals. It has already been noted that the average distance between dislocations measured on photomicrographs was found to be 3.5μ in agreement with previously published data. This corresponds to a dislocation density of about 10^7 per cm^2 and is in excellent agreement with the values for d calculated above. It therefore appears that dislocations are indeed present in the material studied in a density sufficient to account for the observed "average" diffusion coefficients.

6.3. Reappraisal of Previous Results

To explain why the existence of dislocation-influenced diffusion in MgO has not been recognised in

previous work, it should be noted that the ratio of grain boundary diffusion coefficients to lattice diffusion coefficients appears to be much smaller for ionic materials than for metals (Wuensch and Vasilos, 1966b). Furthermore, the extent of diffusion enhancement in grain boundaries seems to depend on impurity precipitation. If these results can be carried over to dislocation diffusion, then this may be unresolvable from lattice diffusion for values of $\sqrt{D_\ell t}$ greater than 10μ say. That is, under these circumstances the difference between the slopes of the two parts of the "average" $(\text{ierfc})^{-1}$ F(x) vs. x graph may be less than the error inherent in the measurement of these slopes. In particular, the autoradiographic method used for the measurement of Ca diffusion appears to have a resolution of about 20μ due in part to the error introduced in scanning. Detection of the existence of the two regions in the diffusion profile would then be unlikely. Even the electron microbeam probe technique may be unsuitable since fluorescence effects have been suspected of reducing the resolution from the normal 1-2μ to something of the order of 10μ (Wuensch and Vasilos, 1966a) when the system studied involves a light matrix such as MgO. Referring to the scatter of reported results for Ca diffusion in MgO at 1300°C, it is tempting to speculate that this arises from a value close to unity for the ratio $D_{\ell + d}/D_\ell$ at this temperature. The point at which intrinsic ("lattice") diffusion

takes over may well vary slightly for MgO from different sources due to differences in either dislocation density or purity, or both. Until considerably more data are available, however, further conjecture along these lines would be of little value.

In the light of the above work, it is interesting to look again at the results of previous work on diffusion in MgO. In the earliest work on Ni^{2+} diffusion in MgO (Wuensch and Vasilos, 1961) the temperature range covered was 1600-1850°C and an activation energy of 4.3 eV was reported. Later when the temperature range was extended down to 1000°C this result was discarded as erroneously high, and the new value for Q quoted as 2.10 eV. Rungis (1965) repeating the nickel measurements using an autoradiographic method in the temperature range 1450°-1600°C again found a Q of about 4 eV and a D_o within an order of magnitude of 10 cm^2/sec, but offered no comment on this. These results indicate that in the case of Ni diffusion in MgO, a lattice diffusion mechanism predominates at temperatures higher than 1500°C.

Tentative data obtained recently (Wuensch and Vasilos, 1966a) has indicated that for Ca diffusion in MgO, Q is 3.3 eV and D_o, 0.025 $cm^2\ sec^{-1}$. These figures are much higher than those obtained by Rungis and Mortlock, as mentioned previously, but are very close to those derived for the lattice diffusion

of Ba in MgO reported in this work. Before going further, it is natural to ask if the reported Q of 3.43 eV for cation self-diffusion in MgO given by Lindner and Parfitt (1957) is truly a lattice diffusion parameter. The answer to this is indicated by the statement made by these authors in which they noted that "some evidence has been found that at temperatures below 1400°C, the (log D vs. 1/T) curve shows a kink with a lower activation energy at low temperatures". It is worth noting that the activation energy of 3.43 eV was quoted for temperatures in the range 1400-1600°C. Confirmation of the existence of a lower activation energy process was found in the conductivity work of Mitoff which indicates a value of 2.17 eV for magnesium ion motion at lower temperatures, and 3.5 eV at high temperatures. Reference has already been made to these results in Chapter I. Also, applying equation (6-3) to self-diffusion requires a value of unity for C_d/C_o. Hence the measured average D will be closer to the lattice D than would be the case for impurity diffusion. It seems reasonable therefore to attribute the value of 3.43 eV for the cation self-diffusion activation energy to a lattice mechanism, operating predominantly above 1400°C.

For diffusion in metals, dislocation diffusion is believed to proceed with an activation energy of half that for lattice diffusion and yields a low value for the pre-exponential term. Q for substitutional diffusion of

impurities in metals, is about equal to that for self-diffusion. The parameters obtained for diffusion in MgO are summarised in Table 6.1. Above the horizontal line are the results obtained which are considered to apply to dislocation influenced diffusion, Those below the line are higher values, some of which are approximate due to the scarcity of results, which could be representative of true lattice diffusion. The relation between these sets of results is in agreement with the qualitative remarks made above based on experience with diffusion in metals.

In view of the influence of dislocations on the diffusion parameters quoted, it is difficult to justify the correlation referred to in the Introduction. Even if it were valid for dislocation diffusion of impurities in MgO (measured over the temperature range 1000-1700°C), its derivation relies on the activation energy for magnesium self-diffusion. This was obtained only for the upper end of the temperature range and is in all likelihood an activation energy for lattice diffusion. In addition, neither of the values of Q for Ba, nor that for Be, agree with the predictions of the correlation. It is considered more valid at this stage, to conclude that the activation energies for all ions diffusing by a dislocation enhanced mechanism in MgO do so with an activation energy in the range 1.6 - 2.1 eV and that lattice diffusion requires activation energies in the range 3.0 - 4.3 eV.

TABLE 6.1

Diffusing Species	Q(eV)	D_o(cm^2/sec)	Reference
Ni^{2+}	2.10	1.80×10^{-5}	Wuensch & Vasilos (1962)
Co^{2+}	2.06	5.78×10^{-5}	"
Fe^{2+}	1.81	8.83×10^{-5}	"
Zn^{2+}	1.85	1.48×10^{-5}	Wuensch & Vasilos (1965)
Ca^{2+}	2.13	2.95×10^{-5}	Rungis & Mortlock (1966)
Be^{2+}	1.60	1.41×10^{-5}	Harding & Mortlock (1966)
Ba^{2+}	1.85	6.3×10^{-5}	Harding (1967)
Mg^{2+}	2.17	-	* Mitoff (1962)
Mg^{2+}	3.5	-	* Mitoff (1962)(high temperature limit)
Mg^{2+}	3.43	0.249	Lindner & Parfitt (1957)
Ni^{2+}	4.3	-	Wuensch & Vasilos (1961)
Ni^{2+}	≈ 4	≈ 10	Rungis (1965)
Ca^{2+}	3.3	0.025	Wuensch & Vasilos (1966)
Ba^{2+}	3.38	0.07	Harding (1967)

* from conductivity measurements

VII. CONCLUSION

Results obtained for the diffusion of Be^{2+} and Ba^{2+} in MgO do not agree with the predictions of a previously formulated correlation. Furthermore, the results of the investigation using ^{133}Ba indicate that over the temperature range 1000-1700°C dislocations strongly influence the observed diffusion coefficients. Evidence for this can be summarised as follows:-

1. Two mechanisms of diffusion operate in the case of Ba in MgO, one being characterised by a very low D_o and an activation energy equal to about half that for cation self diffusion. The second has "normal" values for these parameters.
2. Some previous experiments on impurity diffusion in MgO show values for Q and D_o which are characteristic of dislocation-influenced diffusion.
3. Measurements on the diffusion of Ni in MgO at temperatures over 1450°C, and recent experiments with Ca in MgO all point to the existence of two processes, and again we find both "normal" and "anomalous" values for D_o and Q.
4. Dislocation densities calculated from measured diffusion coefficients are found to be in agreement with those observed in photomicrographs.

This throws doubt on the validity of the correlation of Q with r/α, but before an alternative can be found, considerable work will have to be done to obtain diffusion coefficients which reliably describe lattice diffusion. This will require diffusion measurements being made at temperatures much closer to the melting point of MgO, where lattice diffusion should predominate over dislocation enhanced diffusion.

REFERENCES

Barr, L.W. & Le Claire, A.D. (1964) Proc.Brit.Ceram.Soc.No.1 (July) 109.

Barr, L.W. & Mundy, J.N. (1965) "Diffusion in Body Centred Cubic Metals" Metals Park, Ohio; Am.Soc.Mets. p.171.

Bowen, D.H. & Clarke, F.J.P. (1963) Phil.Mag. 8, 1257.

Brown, A.F. & Blackburn, D.A. (1963) Acta.Met. 11, 1017.

Cadek, J. & Janda, E. (1957) Hutnicke Lisky 12, 1008.

(1959) AERE-Trans 840.

Carslaw, H.S. & Jaeger, J.C. (1959) "Conduction of Heat in Solids" Oxford; Clarendon Press, p.485.

Carter, R. & Richardson, F. (1954) Trans.AIME 200, 1244.

Cumming, Miss P.A. & Harrop, P.J. (1965) AERE-Bib 143.

De Bruin, H.J. & Clark, R.L. (1964) Rev.Sci.Insts. 35, 227.

Dekker, A.J. (1962) "Solid State Physics" London; MacMillan, p.93.

Fisher, J.C. (1951) J.Appl.Phys. 22, 74.

Friedel, J. (1964) "Dislocations" Oxford, Pergamon. p.11.

Girifalco, L.A. (1964) "Atomic Migration in Crystals" New York, Blaisdell. p.124.

Haas, C. (1960) J.Phys.Chem.Solids 15, 108.

Harding, B.C. (1967) Submitted for publication.

Harding, B.C. & Mortlock, A.J. (1966) J.Chem.Phys. 45, 2699.

Harrison, L.G. (1961) Trans.Far.Soc. 57, 1191.

Hart, E.W. (1957) Acta.Met. 5, 597.

Himmel, L., Mehl, R.F. & Birchenall, E. (1953) Trans. AIME 197, 827.

Hoffman, R.E. & Turnbull, D. (1951) J.Appl.Phys. 22, 634.

Kelting, H. & Witt, H. (1949) Z.Physik 126, 697.

Kidson, G.W. (1965) "Diffusion in Body Centred Cubic Metals", Metals Park, Ohio; Am.Soc.Metals p.329.

Lang, A.R. & Miles, G.D. (1965) J.Appl.Phys. 36, 1803.

Laurent, J.F. & Benard, J. (1955) Compt.Rend.241(18) 1204.

(1958) J.Chem.Phys.Solids. 7, 218.

Leblans, L.M.L.J. & Verheijke, M.L. (1963/64) Phillips Tech. Rev. 25, 191.

Le Claire, A.D. (1965) "Diffusion in Body Centred Cubic Metals" Metals Park, Ohio; Am.Soc.Metals. p.3.

Le Claire, A.D. (1966) Phil.Mag. 14, 1271.

Letaw, H., Slifkin, L.M. & Portnoy, W.M. (1954) Rev.Sci.Insts. 25, 865.

Levine, E.M., Robbins, C.R. & McMurdie, H.F. (1964) "Phase Diagrams for Ceramists" Columbus, Ohio; Am.Soc.Mets.p.99.

Lindner, R. & Parfitt, G.D. (1957) J.Chem.Phys. 26, 182.

Lundy, T.S., Federer, J.I., Pawel, R.E. & Winslow, F.R. "Diffusion in Body Centred Cubic Metals" Metals Park, Ohio; Am.Soc.Mets. p.35, 377.

Mapother, D.E., Crooks, H.W. & Maurer, R.J. (1950) J.Chem.Phys. 18, 1231.

Mitoff, S.P. (1959) J.Chem.Phys. 31, 1261.

(1962) J.Chem.Phys. 36, 1383.

(1964) J.Chem.Phys. 41, 2561.

Morrison, D.L. (1963/64) Reactor Materials 6(4) 1-10 (50 references)

Mortlock, A.J. (1960) Acta.Met. 8, 132.

(1964) Acta.Met. 12, 675.

Mott, N.F. & Gurney, R.W. (1940) "Electronic Processes in Ionic Crystals" Oxford. p. 14.

Mullen, J.G. (1961) Phys.Rev. 121, 1649.

Oishi, Y. & Kingery, W.D. (1960) J.Chem.Phys. 33, p.480, 905.

Paladino, A.E. & Kingery, W.D. (1962) J.Chem.Phys. 37, 957.

Pappis, J. & Kingery, W.D. (1961) J.Am.Ceram.Soc. 44, 459.

Pauling, L. (1960) "The Nature of the Chemical Bond" New York, Cornell p.514.

Powers, R. & Doyle, M. (1959) J.App.Phys. 30, 514.

Rueda, F. & Dekeyser, W. (1961) J.Appl.Phys. 32, 1799.

Rungis, J. (1965) "The Diffusion of Calcium in Magnesium Oxide" Thesis, Australian National University, Canberra.

Rungis, J. & Mortlock, A.J. (1966) Phil.Mag. 14, 821.

Ruoff, A.L. & Balluffi, R.W. (1963) J.Appl.Phys. 34, 1848.

Shelly, R., Rigby, E.B. & Cutler, I.B. (1962) J.Am.Ceram.Soc. 45, 302.

Shewmon, P.G. (1963) "Diffusion in Solids" McGraw-Hill, p. 5, 140.

Shim, M.T. & Moore, W.J. (1957) J.Chem.Phys. 26, 802.

Slifkin, L.M., Lazarus, D. & Tomizuka, C.T. (1952) J.Appl.Phys. 23, 1032.

Venables, J.D. (1963) J.Appl.Phys. 34, 293.

Vineyard, G.H. (1957) J.Phys.Chem.Solids 3, 121.

Wert, C. (1950) Phys.Rev. 79, 601.

Wert, C. & Zener, C. (1949) Phys.Rev. 76, 1169.

Wuensch, B.J. & Vasilos, T. (1961) Proc. 4th Int. Sym. "Reactivity of Solids", Amsterdam 1960. (Princeton, N.J., Elsevier) p.57.

Wuensch, B.J. & Vasilos, T. (1962) J.Chem.Phys. 36, 2917.

(1964) J.Am.Ceram.Soc. 47, 63.

(1965) J.Chem.Phys. 42, 4113.

(1966a) Summary Report Mar.1, 1965-Feb.28 1966, Contract No.Nonr-4267(00).

(1966b) J.Am.Ceram.Soc. 49, 433.

Zaplatynsky, I. (1962) J.Am.Ceram.Soc. 45, 28.

(1964) J.Appl.Phys. 35, 1358.